iScience

CellPress
OPEN ACCESS

Article

Environmental and Intestinal Phylum *Firmicutes* Bacteria Metabolize the Plant Sugar Sulfoquinovose via a 6-Deoxy-6-sulfofructose Transaldolase Pathway

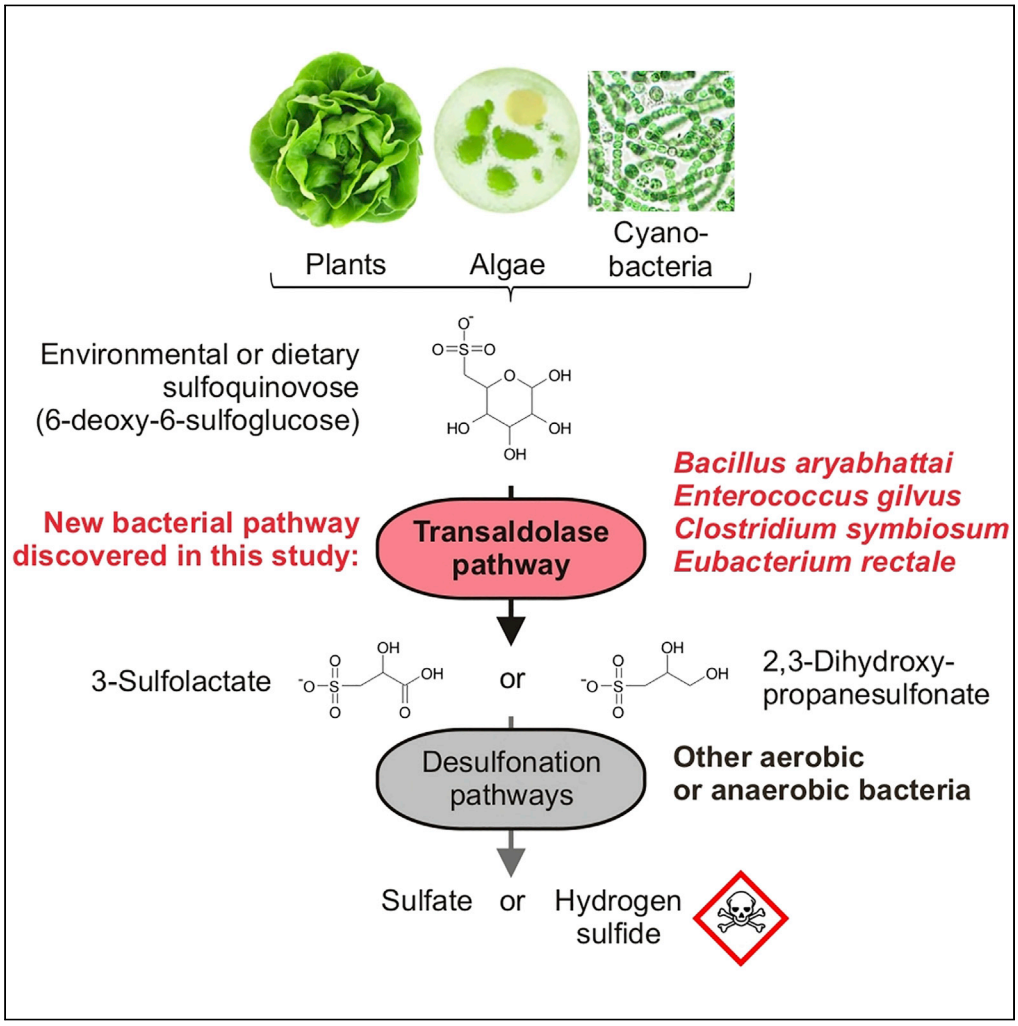

Benjamin Frommeyer, Alexander W. Fiedler, Sebastian R. Oehler, ..., Paolo Franchini, Dieter Spiteller, David Schleheck

david.schleheck@uni-konstanz.de

HIGHLIGHTS

First known SQ-degradation pathway in phylum *Firmicutes* (Gram-positive) bacteria

New enzyme, sulfofructose:D-glyceraldehyde-3-phosphate glyceronetransferase

SQ fermentation pathway in human gut *Enterococcus*, *Clostridium*, and *Eubacterium* strains

Novel degradation route for green-diet SQ to H_2S by intestinal microbial communities

Frommeyer et al., iScience *23*, 101510
September 25, 2020
https://doi.org/10.1016/j.isci.2020.101510

iScience

CellPress
OPEN ACCESS

Article

Environmental and Intestinal Phylum *Firmicutes* Bacteria Metabolize the Plant Sugar Sulfoquinovose via a 6-Deoxy-6-sulfofructose Transaldolase Pathway

Benjamin Frommeyer,[1,2] Alexander W. Fiedler,[1] Sebastian R. Oehler,[1] Buck T. Hanson,[3] Alexander Loy,[3] Paolo Franchini,[1] Dieter Spiteller,[1,2] and David Schleheck[1,2,4,*]

SUMMARY

Bacterial degradation of the sugar sulfoquinovose (SQ, 6-deoxy-6-sulfoglucose) produced by plants, algae, and cyanobacteria, is an important component of the biogeochemical carbon and sulfur cycles. Here, we reveal a third biochemical pathway for primary SQ degradation in an aerobic *Bacillus aryabhattai* strain. An isomerase converts SQ to 6-deoxy-6-sulfofructose (SF). A novel transaldolase enzyme cleaves the SF to 3-sulfolactaldehyde (SLA), while the non-sulfonated C_3-(glycerone)-moiety is transferred to an acceptor molecule, glyceraldehyde phosphate (GAP), yielding fructose-6-phosphate (F6P). Intestinal anaerobic bacteria such as *Enterococcus gilvus*, *Clostridium symbiosum*, and *Eubacterium rectale* strains also express transaldolase pathway gene clusters during fermentative growth with SQ. The now three known biochemical strategies for SQ catabolism reflect adaptations to the aerobic or anaerobic lifestyle of the different bacteria. The occurrence of these pathways in intestinal (family) *Enterobacteriaceae* and (phylum) *Firmicutes* strains further highlights a potential importance of metabolism of green-diet SQ by gut microbial communities to, ultimately, hydrogen sulfide.

INTRODUCTION

6-Deoxy-6-sulfoglucose (sulfoquinovose, SQ) is the polar head group of the plant sulfolipids sulfoquinovosyl diacylglycerols (SQDGs) (Benson, 1963). These lipids are constituents of photosynthetically active membranes in, essentially, all phototrophic organisms (Benning, 1998). Furthermore, certain archaea contain SQ in their surface-layer glycoproteins (Meyer et al., 2011). More on the role of SQ in the biosphere can be found in a recent review (Goddard-Borger and Williams, 2017). Microbial degradation of the large amounts of SQ produced by phototrophs is an important yet largely understudied part of the biogeochemical sulfur cycle (Denger et al., 2012, 2014; Felux et al., 2015; Burrichter et al., 2018). SQ is introduced into the digestive systems of all herbivores and omnivores through their green-vegetable diet and, thus, SQ may be utilized as a substrate also by intestinal microbes (Burrichter et al., 2018).

Complete degradation (mineralization) of the SQ into, ultimately, inorganic sulfate (Denger et al., 2012, 2014) or hydrogen sulfide (Burrichter et al., 2018) can be achieved in two tiers by bacterial communities through metabolite cross-feeding. In the first tier, bacteria catalyze a primary degradation of SQ to C_3-organosulfonates, either 3-sulfolactate (SL) or 2,3-dihydroxypropane-1-sulfonate (DHPS). Such a primary SQ-degradation pathway is the subject of this study. In the second tier, SL- and DHPS-mineralizing bacteria release the inorganic sulfur. Notably, specialized anaerobic bacteria can utilize these SQ degradation intermediates (SL and DHPS) for sulfite respiration (e.g., some *Desulfovibrio* and *Bilophila* spp.) producing potentially harmful hydrogen sulfide (H_2S) (Burrichter et al., 2018), which implies that a complete, anaerobic two-step degradation of SQ to H_2S may be a trait of the intestinal microbiota that is relevant to human health (see ref. Burrichter et al., 2018 and Discussion).

We have previously described two types of biochemical pathways (depicted in Figure 1A) for a primary degradation of SQ to DHPS or SL, in *Escherichia coli* K-12 and *Pseudomonas putida* SQ1, respectively (Denger et al., 2014; Felux et al., 2015).

[1]Department of Biology, University of Konstanz, 78457 Konstanz, Germany

[2]Konstanz Research School Chemical Biology (KoRS-CB), University of Konstanz, 78457 Konstanz, Germany

[3]Division of Microbial Ecology, Centre for Microbiology and Environmental Systems Science, University of Vienna, 1090 Wien, Austria

[4]Lead Contact

*Correspondence: david.schleheck@uni-konstanz.de

https://doi.org/10.1016/j.isci.2020.101510

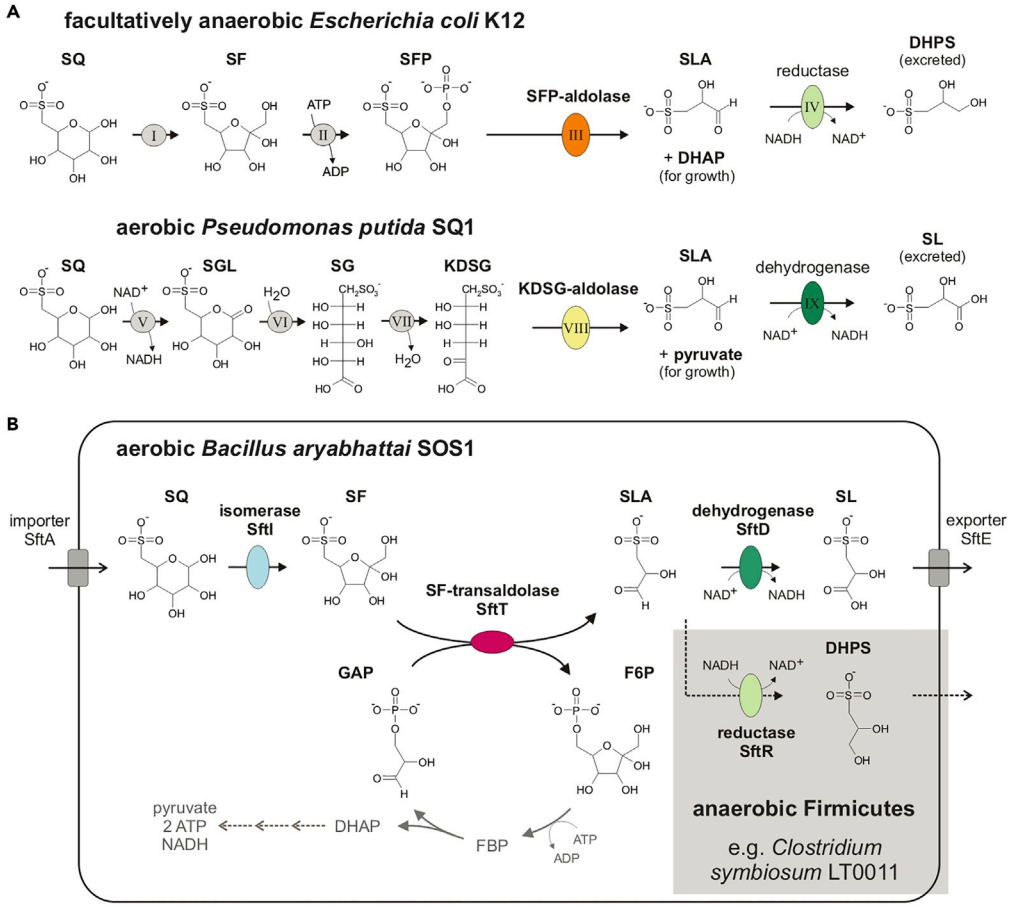

Figure 1. Pathways for Primary SQ Degradation in Bacteria

Illustration of (A) the two known SQ-degradation pathways in *Escherichia coli* K12 and *Pseudomonas putida* SQ1, respectively, and (B) the third SQ-degradation pathway identified in this study in aerobic *Bacillus aryabhattai* SOS1 and in strictly anaerobic, SQ-fermenting bacteria such as *Clostridium symbiosum* LT0011. (A) *E. coli* uses an SQ-Embden-Meyerhof-Parnas (sulfo-EMP) pathway for acquisition of carbon and energy from SQ under both aerobic (Denger et al., 2014) and fermentative growth conditions (Burrichter et al., 2018). It employs a 6-deoxy-6-sulfofructose-1-phosphate (SFP) aldolase (indicated in orange), and it excretes 2,3-dihydroxypropanesulfonate (DHPS) as degradation product during growth with SQ. *P. putida* uses an SQ-Entner-Doudoroff (sulfo-ED) pathway (Felux et al., 2015). It employs a 2-keto-3,6-dideoxy-6-sulfogluconate (KDSG) aldolase (yellow), and it excretes 3-sulfolactate (SL) as degradation product during growth with SQ. See the main text (Introduction) for more detailed descriptions of the pathways and of the abbreviations used for intermediates and enzymes (roman numerals). (B) In this study, a third pathway for SQ was discovered in *B. aryabhattai* SOS1, which excretes SL during SQ degradation. It employs a newly discovered 6-deoxy-6-sulfofructose (SF) transaldolase enzyme (red) that derives fructose-6-phosphate (F6P) for growth (or sedoheptulose-7-phosphate [S7P]; not depicted in Figure 1B) through transfer of the non-sulfonated C3-(glycerone) moiety of SF onto GAP as acceptor molecule (or erythrose-4-phosphate [E4P]; not depicted in Figure 1B). The pathway was identified by differential proteomics to be present also in SQ-fermenting, human gut bacteria, for example, in *C. symbiosum* LT0011, which excretes DHPS during SQ fermentation.

Escherichia coli K-12 catalyzes an SQ-degradation pathway analogous to the Embden-Meyerhof-Parnas (EMP) pathway for glucose-6-phosphate (thus, an sulfo-EMP pathway) under aerobic (Denger et al., 2014) as well as fermentative growth conditions (Burrichter et al., 2018). The sulfo-EMP pathway starts with an aldose/ketose isomerase (enzyme I in Figure 1A; YihS) converting SQ to 6-deoxy-6-sulfofructose (SF), which is phosphorylated by an ATP-dependent SF kinase (enzyme II in Figure 1A; YihV) to 6-deoxy-6-sulfofructosephosphate (SFP). The SFP is then cleaved by an SFP aldolase (enzyme III in Figure 1A; YihT) into 3-sulfolactaldehyde (SLA) and dihydroxyacetone phosphate (DHAP) (Denger et al., 2014). The DHAP supports energy conservation and growth, whereas the SLA cannot be catabolized further but is reduced via an NADH-dependent SLA reductase (enzyme IV in Figure 1A; YihU) to DHPS, which is excreted

(Denger et al., 2014). Notably, this SLA reduction step is beneficial for anaerobic, SQ-fermenting *E. coli* as an additional fermentation step to recover NAD^+ (Burrichter et al., 2018). The sulfo-EMP gene cluster is part of the core genome of commensal and pathogenic *E. coli* strains and can also be found in genomes of other facultatively anaerobic *Enterobacteriaceae* that can thrive in the gastrointestinal tract, e.g., *Salmonella, Klebsiella, Cronobacter*, and *Citrobacter* spp. (Denger et al., 2014; Burrichter et al., 2018). Hence, until today, metabolism of dietary SQ by *Enterobacteriaceae* via the sulfo-EMP pathway has been considered most relevant in intestinal microbiomes of herbivorous animals and humans (Denger et al., 2014; Burrichter et al., 2018), although this has never been assessed *in situ*.

Aerobic *Pseudomonas putida* SQ1 catalyzes a second pathway, analogous to the Entner-Doudoroff (ED) pathway for glucose-6-phosphate (thus, an sulfo-ED pathway) (Felux et al., 2015). The corresponding gene cluster was found in genomes of a wide range of aerobic and nitrate-reducing (respiring) terrestrial, freshwater, and marine Proteobacteria (Felux et al., 2015). Starting with an NAD^+-dependent SQ dehydrogenase (in Figure 1A, enzyme V), the SQ is oxidized to 6-sulfogluconolactone (SGL). The lactone is hydrolyzed by an SGL lactonase (enzyme VI) to 6-deoxy-6-sulfogluconate (SG), which is converted by an SG dehydratase (enzyme VII) to 2-keto-3,6-deoxy-6-sulfo-gluconate (KDSG). The KDSG is then cleaved by a KDSG aldolase (enzyme VIII) into pyruvate and SLA. The pyruvate supports energy conservation and growth. The SLA is also not catabolized further but, in contrast to its reduction to DHPS as in *E. coli*, is oxidized by a NAD^+-dependent SLA dehydrogenase (enzyme IX in Figure 1A) to SL, which is excreted. Notably, this SLA oxidation step is beneficial for respiring bacteria, in order to gain an additional NADH (Felux et al., 2015).

In this study, we revealed a third pathway for primary SQ degradation in a newly isolated aerobic bacterium, *Bacillus aryabhattai* SOS1, which represents the first known SQ-utilizing Gram-positive (phylum *Firmicutes*) bacterium. The pathway was identified by differential proteomics and reconstituted by heterologously produced enzymes, and all key intermediates were identified by mass spectrometry, using $^{13}C_6$-isotopically labeled SQ as substrate. Additionally, we isolated an anaerobic, SQ-fermenting strain, *Clostridium symbiosum* LT0011, from human feces, and we demonstrate that this strain and two common human gut bacteria, *Enterococcus gilvus* DSM15689 and *Eubacterium rectale* DSM17629, harbor and express the newly discovered pathway during SQ fermentation. Hence, metabolism of dietary SQ in intestinal microbiomes may be catalyzed by members of the family *Enterobacteriaceae* via the known sulfo-EMP pathway, as well as by members of the phylum *Firmicutes* via the SQ pathway discovered in this study.

RESULTS

Isolation and Examination of an SQ-Degrading *Bacillus aryabhattai* Strain

Sulfo-EMP and sulfo-ED pathway gene clusters can be found frequently in genomes of Proteobacteria but not in Gram-positive (phylum *Firmicutes*) bacteria. Therefore, we started new aerobic enrichment cultures with SQ as sole carbon and energy source (Denger et al., 2012; Felux et al., 2015) and using soil samples, pond water, or plant leaves as inocula. Replicate soil inocula were pasteurized in order to aid in the enrichment of spore-forming Firmicutes. All enrichments grew, degraded SQ as confirmed by HPLC, and were sub-cultivated until pure cultures were obtained, which were identified by 16S rRNA gene sequencing. From the unpasteurized samples, proteobacterial strains of *Pseudomonas* sp. (plant leaf), *Rhanella* sp. (non-pasteurized soil), and *Aeromonas* sp. (pond) were obtained but not examined further, as they degrade SQ most likely via one of the previously investigated SQ pathways (Figure 1A). However, one of the unpasteurized enrichments (maple leaf) yielded a *Bacillus sp.* strain (termed strain SOS1) with a 16S rRNA gene sequence identity of 99.9% to the *B. aryabhattai* type strain. Two more *Bacillus* sp. strains (strains AF1 and AF2) were isolated from the pasteurized soil enrichment cultures. They utilized the substrate SQ concomitantly with stoichiometrical SL excretion, as determined by HPLC during growth experiments (a linearized growth plot is shown for strain SOS1 in the Supplementary files, Figure S1), but they did not excrete DHPS or sulfate.

We chose *B. aryabhattai* SOS1 (deposited as DSM 104036) as our model organism for further examination of its SQ-degradation pathway. Cell extracts of SQ-grown cells were examined for enzyme activities and metabolites of the two known SQ-degradation pathways, under the reaction conditions used previously (Denger et al., 2014; Felux et al., 2015). Upon addition of SQ, formation of SF was detectable by HPLC-MS (see below), indicative of an SQ isomerase activity. However, addition of known co-substrates (see Figure 1A, ATP and/or NAD^+) yielded no traces of the key intermediate(s) of the sulfo-EMP pathway (SFP;

Figure 1A) (Denger et al., 2014) nor of the sulfo-ED pathway (SG, KDSG; Figure 1A) (Felux et al., 2015). We concluded that strain SOS1 may harbor a different pathway that branches from the sulfo-EMP pathway at the level of SF as first intermediate. Furthermore, the SQ isomerase activity was not detectable in cell extract of glucose-grown cells, suggesting that also this SQ pathway is inducibly expressed (Denger et al., 2014; Felux et al., 2015).

Identification of a Metabolic Gene Cluster that Is Highly Expressed during SQ Degradation in *B. aryabhattai* SOS1

An annotated draft-genome sequence of strain SOS1 was generated for proteomics using Illumina HiSeq sequencing and JGI's Integrated Microbial Genomes (IMG) annotation pipeline (Felux et al., 2015; Burrichter et al., 2018); the annotation is available at IMG (GOLD Analysis Project Id, Ga0111075). Two-dimensional protein gel electrophoresis (2D-PAGE) as well as total proteomics were performed (Figure 2) for extract of cells grown with SQ in comparison with cells grown with glucose, in order to identify the inducible pathway enzymes/genes (e.g., Denger et al., 2014; Felux et al., 2015; Burrichter et al., 2018). For the 2D-PAGE (Figure 2A), all major protein spots visible only for SQ-grown cells, indicative of abundant proteins specifically induced during growth with SQ, were excised and identified by peptide fingerprinting-mass spectrometry. These results were confirmed by the total proteomic analyses (Figure 2B).

Six identified, strongly produced proteins (Figure 2A) were encoded in the same cluster (Figure 2C), for which the predicted proteins/genes had been auto-annotated by the IMG pipeline as follows (gene numbers; the IMG locus tag prefix, Ga0111075_1003, is omitted): 1319 as predicted MFS-type sugar:cation symporter; 1320 as predicted transaldolase; 1321 as protein domain of unknown function (DUF4867) gene; 1322 as glucoside hydrolase (*alpha*-glucosidase); 1323 as aldose/ketose isomerase; 1324 as transcriptional regulator (GntR family); 1325 as aldehyde dehydrogenase; and 1326 as predicted sulfite/organosulfonate exporter (TauE-type) (Figure 2C). The total proteomic analysis (Figure 2B) confirmed a strong expression of these six proteins (Figure 2A), and identified an additional protein (1319) encoded in the same gene cluster, for a predicted glycoside symporter in SQ-grown *B. aryabhattai* SOS1.

Identification of a 6-Deoxy-6-sulfofructose Transaldolase Enzyme in Cell Extracts

The identified, predicted transaldolase 1320 (termed SftT) showed 41.7% amino acid identity (full length) to a characterized fructose-6-phosphate transaldolase (from *Thermoplasma acidophilum*; Lehwess-Litzmann et al., 2011a; Lehwess-Litzmann et al., 2011b) but much lower identity to characterized fructose-6-phosphate aldolases (e.g., from *E. coli*, 25.2%; ref. Schurmann and Sprenger, 2001), suggesting that an acceptor molecule, such as glyceraldehyde-3-phosphate (GAP) or erythrose-4-phosphate (E4P), may be crucial for catalysis. We refined our enzyme reaction conditions (see Transparent Methods) and used gel-filtered cell extract, in which potential co-substrates and acceptor molecules had been removed (size exclusion, >1–5 kDa). Gel-filtered cell extract and SQ alone produced only SF, but a conversion of the SQ via SF further to SLA was detectable after addition of GAP or E4P to the assay, i.e., as acceptor molecules for a transaldolase reaction. Furthermore, with addition of NAD^+ for a predicted SLA dehydrogenase reaction, also a formation of SL was detectable. The transfer of a dihydroxyacetone moiety of SF onto an acceptor molecule by a transaldolase enzyme (glycerone-transferase; EC 2.2.1.2) concomitant with SLA formation (see Figure 1B), as strongly suggested by the results described above, was unequivocally confirmed when we used fully isotopically (^{13}C)-labelled SQ ($^{13}C_6$-SQ) as substrate and when we observed the corresponding mass shifts of the intermediates in MS/MS while the HPLC retention times were unaffected in comparison with authentic, unlabeled standards. As shown in Figure 3, the $^{13}C_6$-SQ was converted to $^{13}C_6$-SF, and through the presence of unlabeled E4P, accumulation of [1,2,3-$^{13}C_3$]-SLA and of [1,2,3-$^{13}C_3$]-sedoheptulose-7-phosphate (S7P) was detectable, and in presence of NAD^+, [1,2,3-$^{13}C_3$]-SL accumulated. Hence, the mass shifts occurring for the molecular-ion of S7P (Figure 3) and its fragmentation products (see Figure S2) identified $^{13}C_6$-labeled SF as the origin of the transferred C_3-(dihydroxyacetone) moiety. When unlabeled GAP instead of E4P was used together with NAD^+, the reaction products were $^{13}C_3$-SLA and $^{13}C_3$-SL, and [1,2,3-$^{13}C_3$]-hexose phosphates but not [1,2,3-$^{13}C_3$]-S7P (Figure S3), confirming that also GAP served as acceptor for the SF transaldolase reaction.

From the results of these enzyme tests with cell extract (Figures 2, S2, and S3) in combination with the proteomic and genomic results (Figures 2A–2C), we concluded that the SQ catabolic pathway in strain SOS1 involves only three inducible enzymes, as depicted in Figure 1B: the isomerase gene product 1323

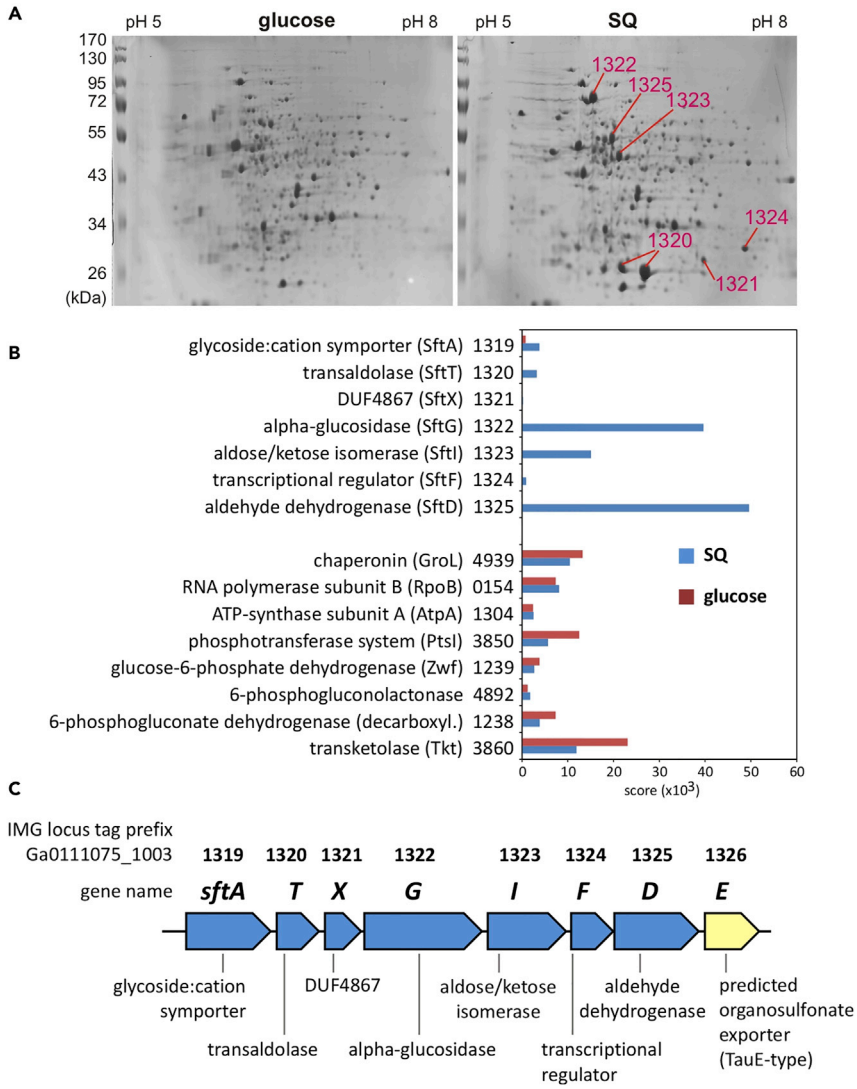

Figure 2. Proteomic Analysis of *B. aryabhattai* SOS1 Cells Identified a Single Gene Cluster for SQ Degradation

(A) Proteins in cell extracts of SQ- or glucose-grown cells were separated via 2D gel electrophoresis (2D-PAGE), and all prominent protein spots visible only for SQ-grown cells were excised and submitted to peptide fingerprinting-mass spectrometry. These spots are labeled according to their IMG gene locus tag numbers (A) and are encoded in the same gene cluster (illustrated in C). The results were replicated once when starting from an independent growth experiment.

(B) Relative abundances of the proteins encoded in this gene cluster as observed by total proteomic analysis in SQ-versus glucose-grown cells. For comparison, the relative abundances of constitutively expressed proteins (GroL, RpoB, AtpA) are also shown, as well as of glucose-inducible enzymes (Entner-Doudoroff/pentose phosphate pathway enzymes). Data from an independent growth experiment and proteomic analysis are shown (n = 1).

(C) Illustration of the identified SQ degradation gene cluster in *B. aryabhattai* SOS1. The locus tag numbers and gene annotations shown refer to the IMG-draft genome annotation of strain SOS1; the IMG locus tag prefix is indicated. These genes were termed *sftATXGIFDE* (6-deoxy-6-sulfofructose transaldolase pathway gene cluster; SFT pathway). The blue coloration indicates genes identified by proteomics (A and/or B).

(Figure 2), catalyzing the interconversion of SQ and SF (Figure 3), and the co-encoded, co-induced transaldolase gene product 1320 (Figure 2), catalyzing the transfer reaction with SF and E4P to SLA and S7P (Figure 3), or with SF and GAP to SLA and F6P (Figure S3). The F6P/S7P powers energy conservation and growth of *B. aryabhattai* SOS1 and serves for regeneration of the corresponding acceptor molecule (as depicted in Figure 1B). The SLA is oxidized to SL (Figures 3 and S3) by the co-encoded, co-induced NAD^+-dependent dehydrogenase 1325 (Figure 2).

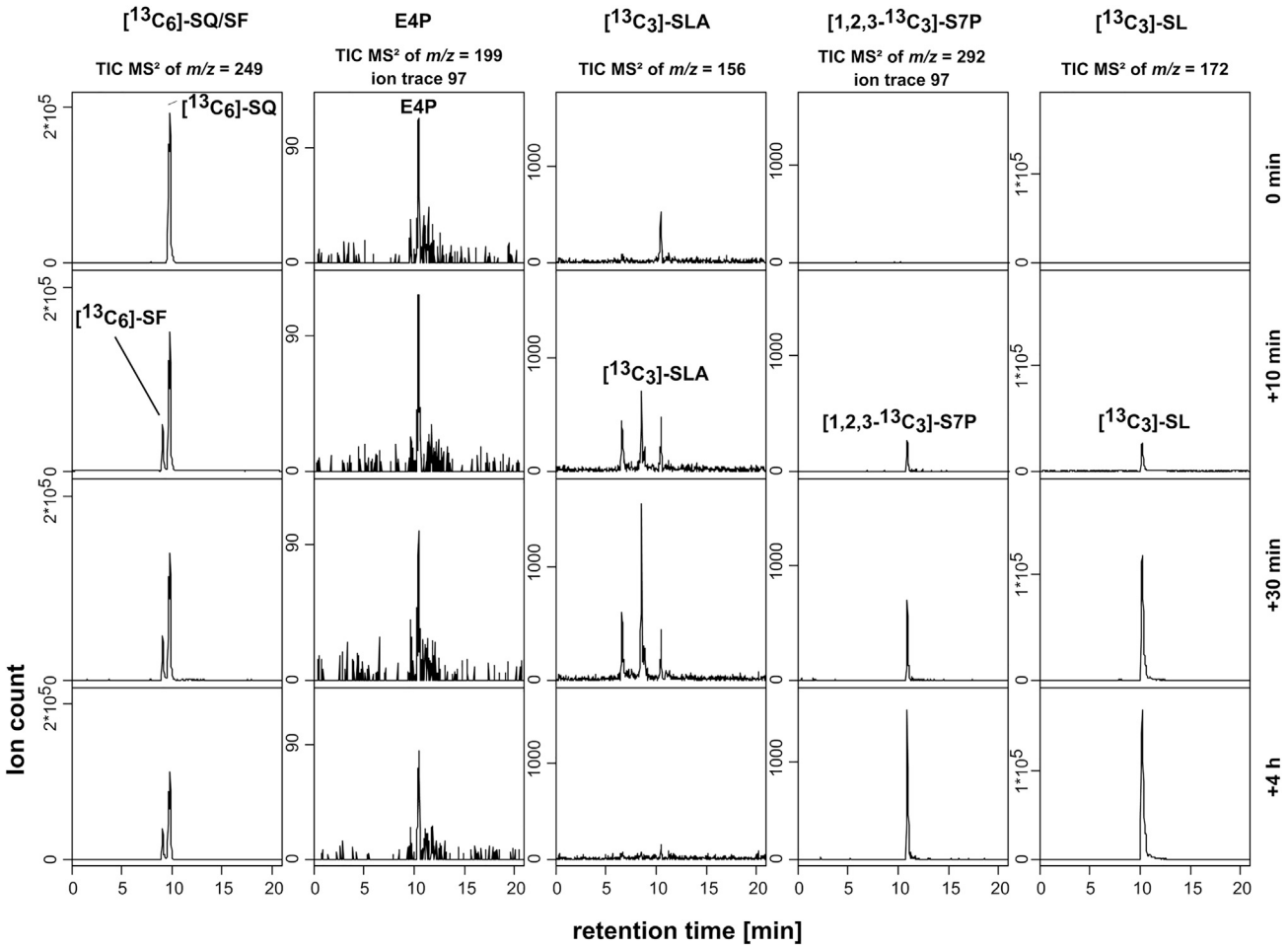

Figure 3. HPLC Mass Spectrometry Confirmed a Transaldolase Reaction in Cell Extracts of SQ-grown *B. aryabhattai* SOS1 Using Fully ^{13}C-Labeled SQ as Substrate and Erythrose-4-Phosphate as Acceptor Molecule

In the presence of unlabeled erythrose-4-phosphate (E4P) and of $^{13}C_6$-SQ, a transient formation of $^{13}C_6$-SF and $^{13}C_3$-SLA, and an accumulation of [1,2,3-$^{13}C_3$]-sedoheptulose-7-phosphate (S7P) and of $^{13}C_3$-SL, was detected. The $^{13}C_3$-SL formation resulted from an SLA dehydrogenase reaction because of the additional presence of NAD^+ in the reaction mixture. The reaction contained 2 mM $^{13}C_6$-SQ, 6 mM E4P (with G6P as impurity; not shown), and 6 mM NAD^+ and was sampled before addition of the gel-filtered cell extract (exclusion, >5 kDa) and after 10, 30, and 240 min of incubation. For the organosulfonates, the total-ion chromatograms (TIC) of the MS/MS-fragmentation of the quasi-molecular ions ($[M-H]^-$) are shown. For the sugar phosphates E4P and [1,2,3-$^{13}C_3$]-S7P, the MS/MS-ion traces of the phosphate group ($[H_2PO_4]^-$, m/z = 97) are shown. Note that $^{13}C_3$-SLA was separated by HPLC as trident peak. The results were replicated twice when starting from independent growth experiments. When E4P was exchanged by GAP as the acceptor, [1,2,3-$^{13}C_3$]-F6P/G6P accumulation was detected (see Figure S3). MS/MS fragmentation mass spectra are shown as Supplementary files for [1,2,3-$^{13}C_3$]-S7P (Figure S2), $^{13}C_6$-SF and $^{13}C_6$-SQ (Figure S5), $^{13}C_3$-SLA (Figure S6), $^{13}C_3$-SL (Figure S7), and E4P (Figure S13).

In Vitro Reconstitution of the SQ-Degradation Pathway

The candidate genes 1320 (*sftT*), 1323 (*sftI*), and 1325 (*sftD*) were cloned into plasmids, heterologously over-expressed in *E. coli*, and the proteins purified via His_6-Tag affinity chromatography (Figure S4). The purified proteins were added sequentially to $^{13}C_6$-SQ-containing reaction mixtures, and samples were taken for HPLC-MS/MS (Figure 4).

With addition of protein 1323 (SftI), formation of a peak showing the same mass as $^{13}C_6$-SQ but a slightly earlier HPLC retention time (Denger et al., 2014) was detected (Figure 4), identified as $^{13}C_6$-SF by its MS/MS fragmentation pattern (Denger et al., 2014) including corresponding ^{13}C mass shifts (see Figure S5). Thus, protein SftI is an SQ isomerase. After addition of protein 1320 (SftT) together with unlabeled GAP as acceptor molecule, $^{13}C_3$-SLA was formed (Figure 4), as identified by its fragmentation pattern (Figure S6) (Felux et al., 2015). Furthermore, [1,2,3-$^{13}C_3$]-F6P formation was observed (Figure 4), confirming that the

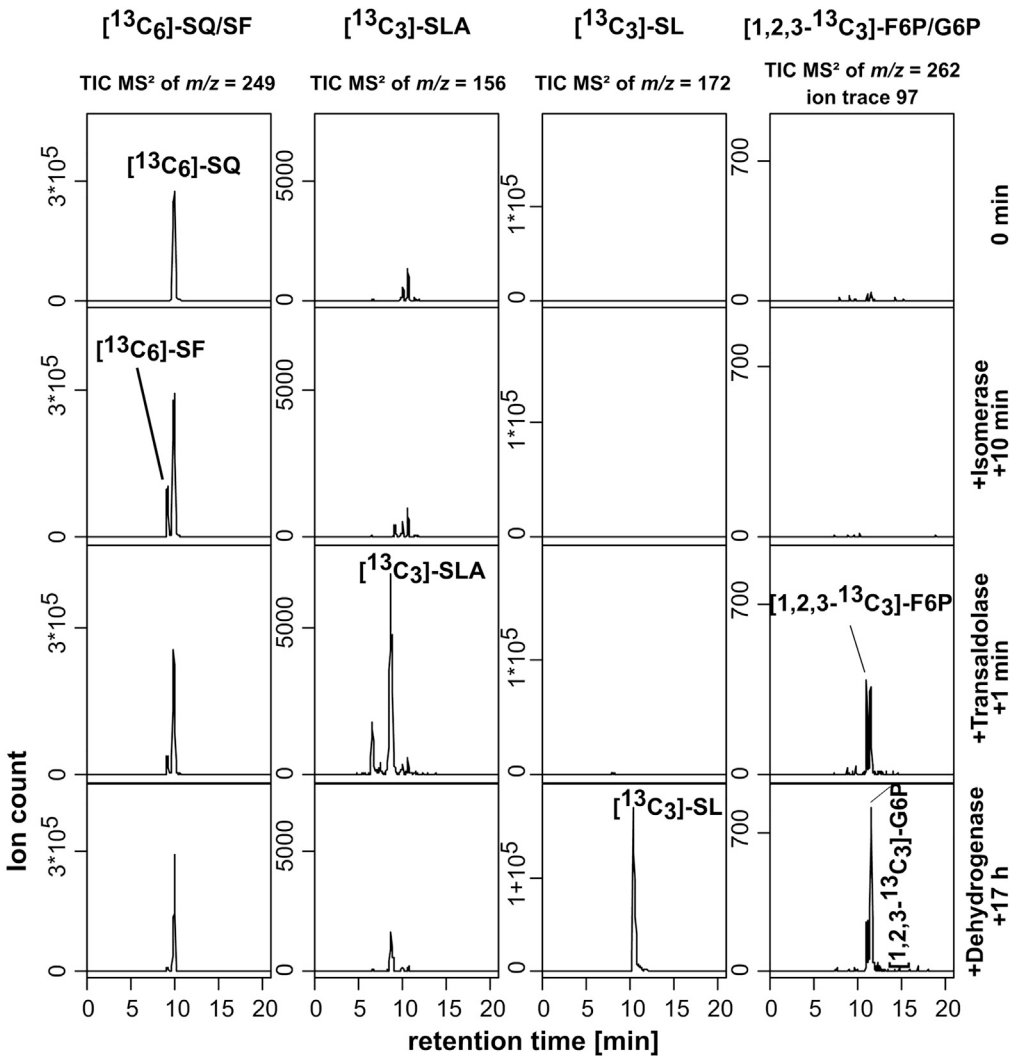

Figure 4. *In Vitro* Reconstitution of the SQ Transaldolase Pathway by Three Recombinant Enzymes

For the organosulfonates, the total-ion chromatograms (TICs) of the MS/MS fragmentation of the quasi-molecular ions ($[M\text{-}H]^-$) are depicted, and for the sugar phosphates F6P and G6P, the characteristic ion traces of the phosphate group ($[H_2PO_4]^-$, m/z = 97). The reaction mixture initially contained 2 mM $^{13}C_6$-SQ and 12 mM GAP (0 min). SQ isomerase SftI (protein 1323) was added (100 μg/mL) and the reaction sampled after 10 min. Then, the SF transaldolase SftT (protein 1320) (50 μg/mL) was added and the reaction sampled after 1 min. Finally, SLA dehydrogenase SftD (protein 1325) (100 μg/mL) and 6 mM NAD^+ was added and the reaction sampled after 17 h. Note that GAP and NAD^+ were added in excess (12 and 6 mM) because the SLA dehydrogenase oxidizes also GAP in the presence of NAD^+; therefore, the SQ conversion was incomplete. Furthermore, the reaction mixture converted the [1,2,3-$^{13}C_3$]-F6P to [1,2,3-$^{13}C_3$]-G6P, owing to an activity of the SQ-isomerase also with F6P. The results were replicated twice using independently produced enzyme preparations. A reaction sequence with E4P instead of GAP as the acceptor is shown in the Supplementary files, Figure S8. A chromatogram depicting the HPLC separation of G6P and F6P in more detail is shown in Figure S11, and MS/MS fragmentation mass spectra for G6P and [1,2,3-$^{13}C_3$]-G6P, and for F6P and [1,2,3-$^{13}C_3$]-F6P, are shown in Figures S12 and S13, respectively.

non-sulfonated $^{13}C_3$-dihydroxyacetone moiety of SQ is transferred onto the unlabeled GAP as acceptor. The enzyme catalyzed the SF-cleavage also with E4P as acceptor, forming $^{13}C_3$-SLA and [1,2,3-$^{13}C_3$]-S7P (see Figure S8), but not with F6P as acceptor. Thus, protein SftT is an SF-cleaving, SLA-forming, GAP/E4P-dependent transaldolase; it showed activity also as sedoheptulose-7-phosphate transaldolase (see Figure S9). Finally, after addition of protein 1325 (SftD) and NAD^+ to the reaction mixture, the $^{13}C_3$-SLA was converted to $^{13}C_3$-SL (Figure 4), as compared with authentic SL standard (Figure S7). Thus, protein

SftD is another NAD^+-dependent SLA dehydrogenase, in addition to the one identified in the *P. putida* sulfo-ED pathway (Figure 1A); SftD oxidized also GAP and E4P as substrates but showed no activity with SL and DHPS, as tested in photometrical assays. Note that specific activities for SLA dehydrogenase could not be determined, because no authentic SLA was available as substrate; the SLA for the enzyme tests was generated in a coupled assay with *E. coli* SLA-reductase (YihU), converting DHPS with NAD^+ to SLA (Felux et al., 2015; Burrichter et al., 2018). Finally, in reaction mixtures in which GAP served as the acceptor (Figure 5), the F6P formed by the SF transaldolase was converted further to G6P, and SQ isomerase SftI was responsible for this activity (see Figure S10).

Enterococcus gilvus, *Clostridium symbiosum*, and *Eubacterium rectale* Strains Employ the SFT Pathway for SQ Fermentation

We searched for bacterial genomes that harbor *sft*-gene clusters using IMG's (https://img.jgi.doe.gov) Ortholog Neighborhood Viewer and Cluster Scout (Hadjithomas et al., 2017) and retrieved a total of 189 candidate clusters, predominantly in members of the classes Bacilli and Clostridia (phylum Firmicutes), e.g., in members of the genera *Bacillus*, *Enterococcus*, *Lactobacillus*, *Butyrivibrio*, *Pseudobutyrivibrio*, *Eubacterium*, and *Clostridium*, and also in individual genomes of members of the phyla Fusobacteria, Chloroflexi, Actinobacteria, Spirochaetes, and Thermotogae. Representative gene-cluster architectures comprising the key genes for enzymes SftITD as well as for SQ-glyceride cleavage of the sulfolipid (SftG, *alpha*-glucosidases), and predicted genes for transport systems (import of SQ and excretion of SL or DHPS), regulation and metabolism of glycerol, if present (Discussion), are illustrated in Figure 5. For a list of all genomes retrieved via IMG (as of 3 July 2020) that contain candidate SFT-gene clusters, see Table S2. For example, we found candidate gene cluster in approximately 1% of all *Bacillus* genomes; hence, the gene cluster may be descriptive of specific ecotypes, e.g., plant or intestine associated, but it is not part of the core genome (pan-genome) of *Bacillus* species, in contrast to the sulfo-EMP pathway gene cluster in *E. coli* (Denger et al., 2014).

Interestingly, the gene clusters of the strictly anaerobic Clostridia encoded, instead of an SLA dehydrogenase (SftD; dark green in Figures 5 and 1A), exclusively an NADH-dependent DHPS-forming SLA reductase (SftR, indicated in light green in Figures 5 and 1A), such as the characterized SLA reductases of *E. coli* (YihU; ref. Denger et al., 2014; Sharma et al., 2020) and of *Desulfovibrio* sp. DF1 (DhpA, physiologically catalyzing the reverse reaction; see ref. Burrichter et al., 2018). This strongly suggested that these strains catalyze an SQ fermentation pathway that may result in DHPS as degradation product, instead of SL, hence, as an additional fermentation step to recover NAD^+, as with the sulfo-EMP pathway of *E. coli* (Figure 1A; ref. Burrichter et al., 2018).

Hence, we additionally confirmed as part of this study for three strictly anaerobic, human-gut Firmicutes strains with *sft*-gene clusters, that they (1) indeed are capable of growing through SQ fermentation and (2) excrete DHPS or SL (Figure 6A) and (3) produce the Sft proteins specifically during growth with SQ, as observed by differential proteomics (Figure 6B). *Enterococcus gilvus* DSM15689 (order Lactobacillales) (Tyrrell et al., 2002) and *Eubacterium rectale* (*Agathobacter rectalis*) DSM17629 (order Clostridiales) (Duncan and Flint, 2008) were examined, and *Clostridium symbiosum* LT0011, which we isolated from human feces by streaking on SQ-containing agar plates and picking of colonies into SQ-containing liquid medium. Strain LT0011 (deposited as DSM108250) was genome sequenced (IMG Genome ID, 2802428835) for the proteomic analysis (Figure 6B); SQ fermentation was confirmed also for *C. symbiosum* type-strain DSM934 (Kaneuchi et al., 1976). For growth of the strains in anaerobic liquid culture, a carbonate-buffered minerals salts medium with Ti(III)NTA as reducing agent (Burrichter et al., 2018) supplemented with SQ (10 mM) and yeast extract (0.1% w/v) was used.

As shown in Figure 6A, *E. gilvus* produced SL but not DHPS during fermentation of SQ under our growth conditions, whereas *C. symbiosum* and *E. rectale* produced DHPS but not SL. The predicted inducible expression of the SFT pathway genes during SQ fermentation was confirmed by the differential proteomics results, as shown in Figure 6B.

DISCUSSION

In this study, we established the first primary SQ-degradation pathway known in the ecologically and industrially important group of Gram-positive (phylum *Firmicutes*) bacteria, by using a newly isolated environmental *B. aryabhattai* strain as model system, by differential proteomics, by *in vitro* reconstruction of the

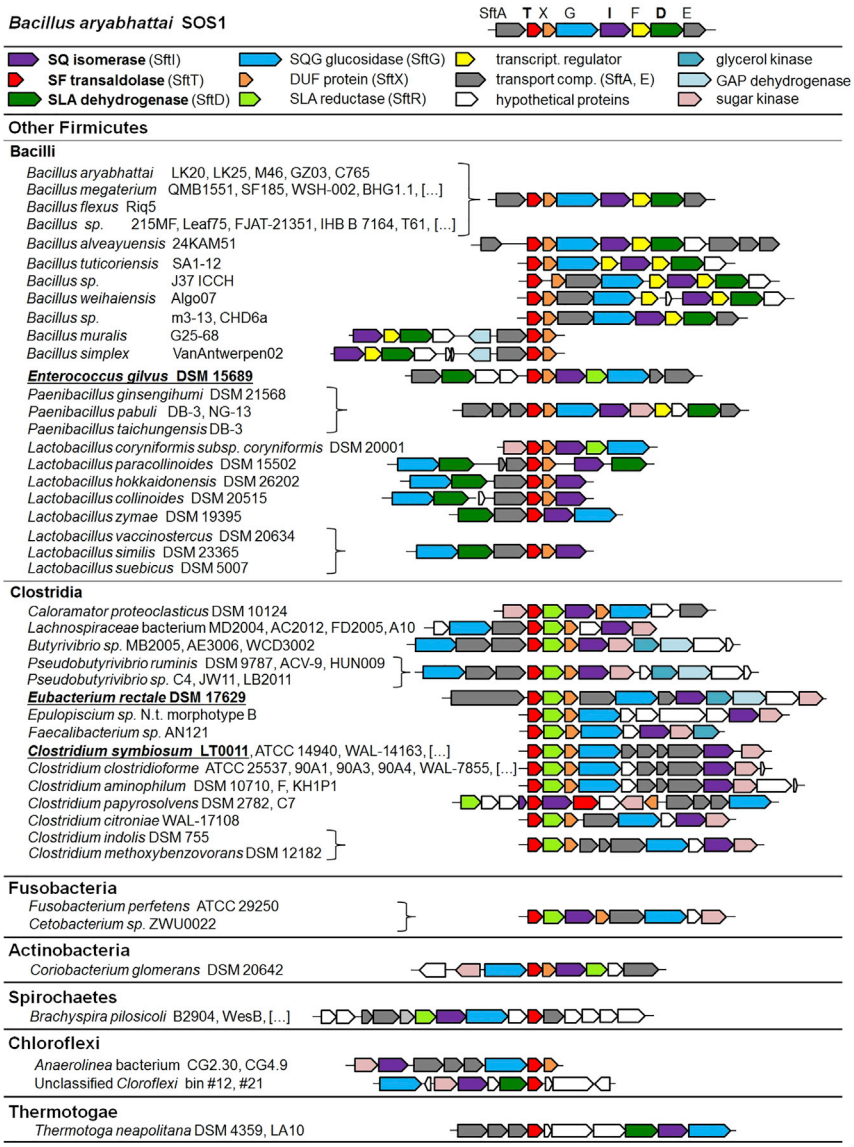

Figure 5. Homologous SF-Transaldolase Pathway Gene Clusters are Found Widespread Particularly in Genomes of Aerobic and Anaerobic (Phylum) Firmicutes (Class) Bacilli and Clostridia

Shown are selected gene-cluster architectures as retrieved from the IMG Ortholog Neighborhood Viewer when using the transaldolase SftT as query. In total, 183 orthologous gene clusters were identified in IMG. The gene clusters shown encode also candidate genes for SQ-glyceride hydrolases (*alpha*-glucosidases), transport systems (import of SQ and excretion of SL or DHPS), and regulation. Importantly, most of the genes clusters of the strictly anaerobic Firmicutes encode SLA reductase candidate genes (termed SftR) homologous to YihU of *E. coli*, instead of SLA dehydrogenases (SftD) genes, suggesting that these strains most likely catalyze an SQ-fermentation pathway that results in DHPS instead of SL as degradation product (see text). Indicated by underlined letters are three representative strains that were examined in this study for their ability to ferment SQ, excrete SL or DHPS, and produce the SFT pathway proteins specifically during growth with SQ, as confirmed by proteomics for all three strains (Figure 6).

pathway with recombinant enzymes, and by identification of all intermediates using fully ^{13}C-labeled SQ as substrate. Surprisingly, homologous pathway gene cluster can be found widespread particularly in genomes of aerobic and anaerobic (phylum) *Firmicutes*, (class) *Bacilli* and *Clostridia*, and also in individual genomes of members of other important bacterial phyla, for example, *Fusobacteria*, *Actinobacteria*, *Spirochaetes*, *Chloroflexi*, and *Thermotogae*. For three representative strains of the strictly anaerobic and

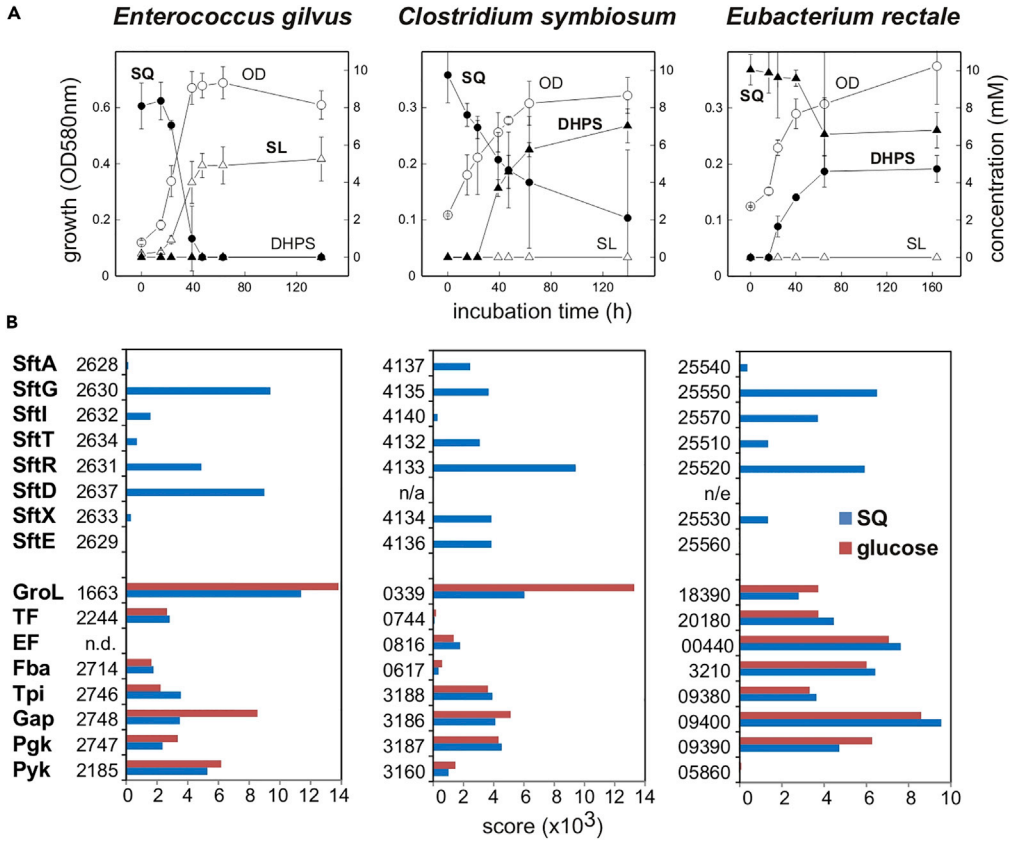

Figure 6. Fermentation of SQ by Human Intestinal Bacteria via the SF-transaldolase Pathway

(A and B) Fermentation of SQ to SL or DHPS by human intestinal bacterial strains *Enterococcus gilvus* DSM15689, *Clostridium symbiosum* LT0011, and *Eubacterium rectale* DSM17629 (A) and proteomic confirmation of a strong, inducible expression of the Sft-proteins during growth with SQ (B). (A) *E. gilvus* produced SL during SQ fermentation and *C. symbiosum* and *E. rectale* produced DHPS but not SL. The used mineral salts medium had to be supplemented with yeast extract (0.1% w/v) for observing growth, and no complete turnover of the SQ provided (10 mM) was obtained, presumably due to depletion of supplements, except for *E. gilvus*. Triplicates (n = 3) are shown; the error bars indicate standard deviations. From replicate cultures, cellular biomass was collected at the end of the growth phase and submitted to total proteomic analyses in comparison to glucose-fermenting cells. (B) Differential proteomics confirmed a strongly inducible expression of the Sft-pathway genes during fermentation of SQ but not when the strains were grown with glucose. Each result was replicated at least once when starting from independent growth experiments. Abbreviations used: SftA, predicted SQ importer; SftG, SQG hydrolase (*alpha*-glucosidase); SftI, SQ isomerase; SftT, SF transaldolase; SftR, SLA reductase; SftD, SLA dehydrogenase; SftX, DUF4867; SftE, predicted SL/DHPS exporter; GroL, chaperon; TF, translation factor; EF, elongation factor; Fba, fructose bisphosphate aldolase; Tpi, triosephosphate isomerase; Gap, GAP dehydrogenase; Pyk, pyruvate kinase; n.d., not detected; n/e, not encoded in the respective *sft*-gene cluster (see Figure 5).

important human-gut (class) *Bacilli* and *Clostridia*, we confirmed their predicted ability to grow with SQ and that they express the pathway enzymes inducibly during fermentative growth with SQ.

Our previous additions to the known glycolytic (monosaccharide degradation) pathways in bacteria were the two "sulfoglycolytic" pathways (Denger et al., 2014; Felux et al., 2015) for catabolism of the 6-sulfo-nated-6-deoxy hexose SQ, which are analogous to the Embden-Meyerhof-Parnas (e.g., Kresge et al., 2005; Barańskaa et al., 2007) and the Entner-Doudoroff (Entner and Doudoroff, 1952) pathways for glucose-6-phosphate (G6P) (Figure 1A), given the structural similarity of the substrates SQ and G6P. All these pathways employ aldolases (aldehyde lyases, EC 4.1.2.x) for cleavage of the C_6-monosaccharides into C_3 fragments. The third bacterial pathway for primary SQ degradation uncovered in this study reminds somewhat of another glycolytic pathway for G6P, the pentose-phosphate pathway (Gunsalus et al., 1955; Horecker, 2002), in that a transaldolase enzyme (aldehyde/ketone transferase, EC 2.2.1.x) is involved in

acquisition of monosaccharide carbon, as depicted in Figure 1B. The SF transaldolase (proposed systematic name, 6-deoxy-6-sulfofructose:D-glyceraldehyde-3-phosphate glyceronetransferase) excises a sulfonated C_3 fragment (SLA), and it acquires a non-sulfonated C_3 fragment from SQ by transferring a glycerone-moiety onto an acceptor molecule, GAP or E4P, yielding F6P or S7P (Figures 3, 4, S3, and S8). The F6P and S7P is used for regeneration of the acceptor and as carbon and energy source for cellular biomass formation (Figure 1B). Differences of the newly discovered SQ pathway to the pentose phosphate pathway, however, are absence of both NADH generation and decarboxylation reaction and, thus, that not a pentose intermediate is cleaved.

The biochemical and genetic identity of this third bacterial pathway for SQ catabolism, as established in this study, is adding to a surprisingly high, but yet mostly underappreciated, diversity of microbial pathways for utilization of organosulfonates, as has probably first been noted for taurine (e.g., Cook and Denger, 2006; see also MetaCyc [https://biocyc.org], taurine degradation I–IV, and Peck et al., 2019). The genetic and biochemical identification of this third SQ pathway is also adding valuable insight, as well as future experimental access, to important questions regarding physiology, enzymology, and pathway energetics of SQ degradation, regarding the environmental microbiology of SQ degradation and its contributions to the biogeochemical carbon and sulfur cycles, and also regarding its potential roles in intestinal microbiomes and for human health.

The glycolytic pathways for G6P are optimized according to their overall thermodynamic and biochemical properties of the pathway, necessity of investing in enzymes (protein) to maintain sufficient pathway fluxes, and their molar yields of energy equivalents (ATP) and reducing equivalents (NADH) relative to the electron acceptors used (e.g., Bar-Even et al., 2012; Flamholz et al., 2013). Given the structural similarity of SQ and G6P, similar energetic and ecophysiological constraints have obviously led to the evolution of also several biochemical strategies for degradation of SQ. However, a common theme for all known SQ-degradation pathways is that the "waste product" SLA is employed either as additional electron donor or as additional electron acceptor (Figure 1). One of the many interesting questions arising is whether the benefits of this type of SLA utilization, either as electron donor or acceptor, might in many environmental settings outweigh the benefit of further catabolizing the SLA-carbon (for example, by desulfonation of SL to pyruvate through sulfolactate sulfo-lyase, SuyAB; ref. Burrichter et al., 2018) and whether this might be an explanation for the division of labor (Tsoi et al., 2018; Giri et al., 2019) observed thus far in complete SQ degradation, that is, primary SQ degradation and cross-feeding of the DHPS or SL to different microorganisms that mediate the desulfonation reactions (Denger et al., 2012, 2014; Burrichter et al., 2018) for closing the sulfur cycle. Further interesting questions are arising around the different forms non-sulfonated C_3-carbon acquired through the three different SQ pathways, that is DHAP by the sulfo-EMP pathway, pyruvate by the sulfo-ED pathway, and a C_3-(glycerone)-moiety incorporated into F6P/S7P by the SFT pathway (Figure 1). Although the yields of reducing equivalents and ATP of the different pathways appear well traceable (see below), the particular benefits and costs of funneling the SQ-carbon into the anabolic reactions and fermentations at these different levels is unclear. For example, the particular advantages of the different SQ-pathway strategies may become fully visible only if degradation of the sulfolipid metabolite SQ-glyceride (SQG) is explored further as substrate, instead of only SQ: every SQ-degradation gene cluster examined thus far co-encodes an SQG glucosidase (sulfoquinovosidase) homolog (SftG in Figures 2 and 5; see also refs. Denger et al., 2014; Felux et al., 2015) for cleaving SQG to SQ and glycerol (Speciale et al., 2016), and every SQ-degrading strain examined thus far by proteomics strongly co-induced this sulfoquinovosidase (Figures 2 and 6B; refs. Denger et al., 2014; Felux et al., 2015; Burrichter et al., 2018; Li et al., 2020). Furthermore, *E. coli* is able to grow with SQG (Abayakoon et al., 2018, and our own observation) as well as *P. putida* SQ1, *B. aryabhattai* SOS1 (our own observations), and SQ-degrading *Rhizobium leguminosarum* SRDI565 (Li et al., 2020). We suggest that for the SFT pathway, the glycerol acquired from SQG cleavage may directly feed into generation of the acceptor molecule GAP for the SF transaldolase, through glycerol kinase and glycerol-3-phosphate dehydrogenase, some of which are co-encoded in the predicted gene clusters (see Figure 5). This needs to be addressed in future, as well as the directly related questions whether indeed SQG rather than SQ might be the more environmentally relevant substrate for SQ-catabolic microorganisms (Abayakoon et al., 2018) and whether the SQG glucosidase gene may be a universal genetic marker for SQ(G) metabolism across all types of pathways.

Overall, the now three known pathways for SQ with either SLA oxidation to SL or its reduction to DHPS, seem to reflect adaptations to the aerobic, facultatively anaerobic, or strictly anaerobic ecophysiology

of the different environmental and intestinal microorganisms. SQ utilization by the SL-producing, aerobic *P. putida* SQ1 through the sulfo-ED pathway inclusive of the SLA dehydrogenase reaction (Figure 1A) (Felux et al., 2015), is represented by the equation

$$SQ + 2\ NAD^+ \rightarrow pyruvate + SL + 2\ NADH + 2\ H^+.$$

The pyruvate-carbon is assimilated and oxidized for energy generation through aerobic respiration, and the two NADH are also driving respiration. SQ utilization by DHPS-producing, facultatively anaerobic *E. coli* K12 through the sulfo-EMP pathway including the SLA reductase reaction (Denger et al., 2014), and including substrate-level phosphorylation of the DHAP released (see Figure 1A), is represented by the equation

$$SQ + ADP + P_i \rightarrow pyruvate + DHPS + ATP.$$

The pyruvate-carbon is also assimilated and oxidized for energy generation through aerobic respiration (Denger et al., 2014), or it is metabolized and reduced as electron acceptor in mixed-acid fermentation (Burrichter et al., 2018), as has been discussed previously (Felux et al., 2015; Burrichter et al., 2018). The SQ utilization by the SL-producing, aerobic *B. aryabhattai* SOS1 through the oxidative SFT pathway including the SLA dehydrogenase reaction, as described in this study, and including of the regeneration of the transaldolase-acceptor molecule and substrate-level phosphorylation of the DHAP acquired from SQ (see Figure 1B), is represented by the equation

$$SQ + 2\ NAD^+ + ADP + P_i \rightarrow pyruvate + SL + 2\ NADH + ATP + 2\ H^+.$$

Hence, as with the sulfo-ED pathway in *P. putida*, this pathway generates NADH for respiration; however, in addition, also one ATP is conserved from DHAP further downstream (see Figure 1B), as with the sulfo-EMP pathway of *E. coli*. Furthermore, the acquisition of the SQ-carbon requires only two enzymes in the SFT pathway, in comparison with the sulfo-ED pathway with four enzymes and the sulfo-EMP pathway with three enzymes (Figure 1). Hence, explanations on the particular advantages of the different SQ-pathway strategies may be provided not only based on pathway energetics and the ATP and NADH yields in relation to the electron acceptor used but also on the level of investment in protein synthesis. Finally, the SQ utilization through the reductive SFT pathway by the fermenting *C. symbiosum* and *E. rectale* strains that encode (Figure 5) and express SLA reductases (Figure 6B) and excrete DHPS (Figure 6A) is represented by the equation

$$SQ + ADP + Pi \rightarrow pyruvate + DHPS + ATP,$$

thus, as with the sulfo-EMP pathway of *E. coli*. However, why *Enterococcus gilvus* DSM15689 is excreting SL instead of DHPS during SQ fermentation under our cultivation conditions (Figure 6A), which is counterintuitive, remains yet unresolved. Note that its gene cluster (Figure 5) encodes both SLA dehydrogenase (SftD) and reductase (SftR) candidates and that both are expressed (Figure 6B). Thus, *E. gilvus* may be able to switch between SL and DHPS production depending on its growth conditions, e.g., in presence of alternative electron acceptors or in dependence on a metabolic partner organism. In addition, future work will also have to corroborate the yet only tentatively identified non-sulfonated fermentation products formed, that is, for *E. gilvus* apparently acetate and formate, and for *C. symbiosum* and *E. rectale* apparently acetate and H_2, but not formate, butyrate, or butanol. Their identification and thorough quantification relative to total biomass formation will establish carbon and electron balances (e.g., Burrichter et al., 2018) and, thus, allow for an overall quantitative, stoichiometrical comparison of the SQ fermentations employing the SFT pathway (Figure 6) relative to that of *E. coli* via the sulfo-EMP pathway (Burrichter et al., 2018). Such detailed examination might also provide answers to the intriguing questions why the sulfo-EMP pathway is especially widespread among *Enterobacteriaceae* (Denger et al., 2014), the sulfo-ED pathway across (other) Proteobacteria (Felux et al., 2015), and why the (oxidative and reductive) SFT pathway(s) are found so prominently across genomes of aerobic as well as anaerobic Gram-positive (phylum *Firmicutes*) bacteria (Figure 5).

Environmental studies of SQ-degrading microorganisms, as well as of SL- or DHPS-degrading microorganisms, are needed to fully reveal their diversity, ecological niches, and significance in the carbon and sulfur cycles in all habitats where SQ is produced and/or degraded. The sulfo-ED pathway genes are found in marine- or saline-associated bacteria (e.g., *Halomonas, Salinarimonas*), freshwater-, soil-, and plant rhizosphere-associated bacteria (e.g. *Microvirga, Ensifer, Herbaspirillum, Rhizobium* strains), and also in

human-gut symbionts (e.g., *Hafnia*, *Leminorella*, and *Serratia* strains) and/or potential pathogens (*Vibrio*, *Plesiomonas*, and *Halomonas* strains). The sulfo-EMP pathway gene cluster is a feature of the *E. coli* core genome and also of other *Enterobacteriaceae* genomes (e.g., *Salmonella*; *Rhanella* sp. isolated in this study) as trait relevant for their intestinal as well as environmental lifestyles. The SFT pathway gene cluster is found (Figure 5) in Firmicutes of the soil and plant environment (e.g., *Bacillus* and *Lactobacillus* strains) and also among strains of the human intestinal tract and rumen of livestock (e.g., *Clostridium*, *Eubacterium*, *Enterococcus*, *Butyrivibrio*, and *Faecalibacterium* strains). Given SQ is a relevant constituent of the green-diet of all herbivores and omnivores (Denger et al., 2014; Goddard-Borger and Williams, 2017) and given the wide distribution of SQ degradation gene clusters in phylogenetically diverse intestinal bacteria, SQ and its degradation products DHPS and/or SL might represent yet unappreciated substrates for the intestinal microbiota of humans and animals. For the primary degradation (fermentation) of SQ, it is probably most interesting to explore whether commensal or pathogenic *Enterobacteriaceae*, or whether intestinal Firmicutes, utilize the dietary SQ. The genetic signatures of these metabolic features are now available, e.g., for their assessments using omics methods. Importantly, organosulfonates such as the SL and DHPS produced from primary SQ degradation can be substrates for sulfite respiration and sulfide (H_2S) production by the intestinal pathobiont *Bilophila wadsworthia* and by *Desulfovibrio* spp. (Burrichter et al., 2018; Peck et al., 2019). H_2S is a key microbial and host-cell-derived metabolite in the intestine and has many detrimental as well as beneficial contributions to human health and disease (e.g., Attene-Ramos et al., 2010; Carbonero et al., 2012; Singh and Lin, 2015; Ijssennagger et al., 2016). Thus, the genetic and biochemical information provided in this study will help to disentangle also effects of diet-derived SQ on the microbiota composition, and on H_2S homeostasis in the gut, each contributing to an improved understanding of the complex interactions between diet, microbiota, and host health (Heintz-Buschart and Wilmes, 2018).

Limitations of the Study

The insights gained via our approach using pure bacterial cultures and classical microbiological and biochemical methods must be complemented with empirical data on SQ degradation processes examined directly in the environment and gut microbiomes, e.g., by omics methods. Hence, environmental studies of SQ-degrading microorganisms, as well as of SL- or DHPS-degrading microorganisms, are urgently needed to fully reveal their diversity, ecological niches, and significance in the carbon and sulfur cycles in all habitats where SQ is produced and/or degraded. A thorough determination of carbon and electron balances and, thus, an overall stoichiometric and energetic comparison of, e.g., the SQ fermentations via the SFT pathway relative to that of *E. coli* via the sulfo-EMP pathway, must also await future, more detailed studies, as well as further descriptions of the enzymes and their kinetic parameters once authentic substrates are available. In summary, our study highlights the importance of establishing the genetic identity of physiological and biochemical features in isolated bacterial strains in the laboratory, for evaluating their role and importance directly in the environment by omics methods. In this case, for adding valuable insight to important questions regarding the environmental microbiology of SQ degradation and its contribution to the biogeochemical carbon and sulfur cycles, and also regarding its potential roles in intestinal microbiomes and for human health.

Resource Availability

Lead Contact

Further information and requests for resources and reagents should be directed to and will be fulfilled by the Lead Contact, Prof. David Schleheck (david.schleheck@uni-konstanz.de).

Materials Availability

Data related to this paper may be requested from the lead author. The bacterial strains isolated and examined in this study were deposited at the Leibniz Institute-German Collection of Microorganisms and Cell Cultures (https://www.DSMZ.de) under reference numbers DSM 104036 for *B. aryabhattai* SOS1 and DSM108250 for *Clostridium symbiosum* LT0011. Their (draft) genome sequences are available at IMG (https://img.jgi.doe.gov), for strain SOS1 under GOLD Project Id. Ga0111075 and for strain LT0011 under IMG Genome Id. 2802428835.

Data and Code Availability

This study did not generate code.

METHODS

All methods can be found in the accompanying Transparent Methods supplemental file.

SUPPLEMENTAL INFORMATION

Supplemental Information can be found online at https://doi.org/10.1016/j.isci.2020.101510.

ACKNOWLEDGMENTS

We like to thank Andreas Marquardt for the proteomic analyses, the AGs Schink and Schleheck, especially Anna Burrichter, Karin Denger, Jasmin Frey, and Sylke Wiechmann for their support, and Bernhard Schink and Valentin Wittmann for fruitful discussions. We also thank Maraike Mühleck and Christof Mayer for their unfortunately unsuccessful attempts for establishing a transformation and knockout system for *B. aryabhatta* SOS1, and we thank Magnus Schmidt and Markus Ringwald. This work was funded by the University of Konstanz, the Konstanz Young Scholar Fund (YSF), the Konstanz Research School Chemical Biology (KoRS-CB), the Austrian Science Fund (FWF project grant I2320-B22), and the Deutsche Forschungsgemeinschaft (DFG grants SCHL1936/3 and 4).

AUTHOR CONTRIBUTIONS

D. Schleheck conceived the study. B.F. did the enzymic and analytical-chemical work. S.R.O. enriched and isolated strain SOS1 and S.R.O. and A.W.F. other aerobic SQ-degrading strains, and they characterized their growth. A.W.F. performed the proteomics and growth experiments with strain SOS1 and the SQ-fermenting strains. P.F. established the strain SOS1 genome. B.F. and D Spiteller performed the HPLC-MS analysis. B.T.H. and A.L. isolated *C. symbiosum* LT0011 and established its genome sequence. B.F. and D. Schleheck wrote the manuscript and all authors revised and approved it.

DECLARATION OF INTERESTS

The authors declare they have no competing interests.

Received: May 2, 2020
Revised: July 4, 2020
Accepted: August 25, 2020
Published: September 25, 2020

REFERENCES

Abayakoon, P., Jin, Y., Lingford, J.P., Petricevic, M., John, A., Ryan, E., Wai-Ying Mui, J., Pires, D.E.V., Ascher, D.B., Davies, G.J., et al. (2018). Structural and biochemical insights into the function and evolution of sulfoquinovosidases. ACS Cent. Sci. *4*, 1266–1273.

Attene-Ramos, M.S., Nava, G.M., Muellner, M.G., Wagner, E.D., Plewa, M.J., and Gaskins, H.R. (2010). DNA damage and toxicogenomic analyses of hydrogen sulfide in human intestinal epithelial FHs 74 Int cells. Environ. Mol. Mutagen. *51*, 304–314.

Bar-Even, A., Flamholz, A., Noor, E., and Milo, R. (2012). Rethinking glycolysis: on the biochemical logic of metabolic pathways. Nat. Chem. Biol. *17*, 509–517.

Barańskaa, J., Dzugajb, A., and Kwiatkowska-Korczakc, J. (2007). Embden-Meyerhof-Parnas, the first metabolic pathway: the fate of prominent polish biochemist Jakub Karol Parnas. Compr. Biochem. *45*, 157–207.

Benning, C. (1998). Biosynthesis and function of the sulfolipid sulfoquinovosyl diacylglycerol. Annu. Rev. Plant Biol. *49*, 53–75.

Benson, A. (1963). The plant sulfolipid. Adv. Lipid Res. *1*, 387–394.

Burrichter, A., Denger, K., Franchini, P., Huhn, T., Müller, N., Spiteller, D., and Schleheck, D. (2018). Anaerobic degradation of the plant sugar sulfoquinovose concomitant with H2S production: *Escherichia coli* K-12 and *Desulfovibrio* sp. strain DF1 as co-culture model. Front. Microbiol. *9*, 2792.

Carbonero, F., Benefiel, A.C., Alizadeh-Ghamsari, A.H., and Gaskins, H.R. (2012). Microbial pathways in colonic sulfur metabolism and links with health and disease. Front. Physiol. *3*, 448.

Cook, A.M., and Denger, K. (2006). Metabolism of taurine in microorganisms: a primer in molecular biodiversity? In Taurine 6, *583*, S.S. Oja and P. Saransaari, eds (Springer), pp. 3–13.

Denger, K., Huhn, T., Hollemeyer, K., Schleheck, D., and Cook, A.M. (2012). Sulfoquinovose degraded by pure cultures of bacteria with release of C3-organosulfonates: complete degradation in two-member communities. FEMS Microbiol. Lett. *328*, 39–45.

Denger, K., Weiss, M., Felux, A.K., Schneider, A., Mayer, C., Spiteller, D., Huhn, T., Cook, A.M., and Schleheck, D. (2014). Sulphoglycolysis in *Escherichia coli* K-12 closes a gap in the biogeochemical sulphur cycle. Nature *507*, 114–117.

Duncan, S.H., and Flint, H.J. (2008). Proposal of a neotype strain (A1-86) for *Eubacterium rectale*. Request for an Opinion. Int. J. Syst. Evol. Microbiol. *58*, 1735–1736.

Entner, N., and Doudoroff, M. (1952). Glucose and gluconic acid oxidation of *Pseudomonas saccharophila*. J. Biol. Chem. *196*, 853–862.

Felux, A.-K., Spiteller, D., Klebensberger, J., and Schleheck, D. (2015). Entner-Doudoroff pathway for sulfoquinovose degradation in *Pseudomonas putida* SQ1. Proc. Natl. Acad. Sci. U S A *112*, E4298–E4305.

Flamholz, A., Noor, E., Bar-Even, A., Liebermeister, W., and Milo, R. (2013). Glycolytic strategy as a tradeoff between energy yield and protein cost. Proc. Natl. Acad. Sci. U S A *110*, 10039–10044.

Giri, S., Waschina, S., Kaleta, C., and Kost, C. (2019). Defining division of labor in microbial communities. J. Mol. Biol. *431*, 4712–4731.

Goddard-Borger, E.D., and Williams, S.J. (2017). Sulfoquinovose in the biosphere: occurrence, metabolism and functions. Biochem. J. *474*, 827–849.

Gunsalus, I.C., Horecker, B.L., and Wood, W.A. (1955). Pathways for carbohydrate metabolism in microorganisms. Bacteriol. Rev. *19*, 79–128.

Hadjithomas, M., Chen, I.A., Ken Chu, K., Huang, J., Ratner, A., Palaniappan, K., Andersen, E., Markowitz, V.M., Kyrpides, N.C., and Ivanova, N.N. (2017). IMG-ABC: new features for bacterial secondary metabolism analysis and targeted biosynthetic gene cluster discovery in thousands of microbial genomes. Nucleic Acids Res. *45*, D560–D565.

Heintz-Buschart, A., and Wilmes, P. (2018). Human gut microbiome: function matters. Trends Microbiol. *26*, 563–574.

Horecker, B.L. (2002). The pentose phosphate pathway. J. Biol. Chem. *277*, 47965–47971.

Ijssennagger, N., van der Meer, R., and van Mil, S.W. (2016). Sulfide as a mucus barrier-breaker in inflammatory bowel disease? Trends Mol. Med. *22*, 190–199.

Kaneuchi, C., Watanabe, K., Terada, A., Benno, Y., and Mitsuoka, T. (1976). Taxonomic study of *Bacteroides clostridiiformis* subsp. *clostridiiformis* (Burri and Ankersmit) Holdeman and Moore and of related organisms: proposal of *Clostridium clostridiiformis* (Burri and Ankersmit) comb. nov. and *Clostridium symbiosum* (Stevens) comb. nov. Int. J. Syst. Evol. Microbiol. *26*, 195–204.

Kresge, N., Simoni, R.D., and Hill, R.L. (2005). Otto Fritz Meyerhof and the elucidation of the glycolytic pathway. J. Biol. Chem. *280*, e3.

Lehwess-Litzmann, A., Neumann, P., Golbik, R., Parthier, C., and Tittmann, K. (2011a). Crystallization and preliminary X-ray diffraction analysis of transaldolase from *Thermoplasma acidophilum*. Acta Crystallogr. Sect. F Struct. Biol. Commun. *67*, 584–586.

Lehwess-Litzmann, A., Neumann, P., Parthier, C., Lüdtke, S., Golbik, R., Ficner, R., and Tittmann, K. (2011b). Twisted Schiff base intermediates and substrate locale revise transaldolase mechanism. Nat. Chem. Biol. *7*, 678–684.

Li, J., Epa, R., Scott, N.E., Skoneczny, D., Sharma, M., Snow, A.J.D., Lingford, J.P., Goddard-Borger, E.D., Davies, G.J., McConville, M.J., and Williams, S.J. (2020). A sulfoglycolytic Entner-Doudoroff pathway in *Rhizobium leguminosarum* bv. *trifolii* SRDI565. Appl. Environ. Microbiol. *86*, e00720–e00750.

Meyer, B.H., Zolghadr, B., Peyfoon, E., Pabst, M., Panico, M., Morris, H.R., Haslam, S.M., Messner, P., Schäffer, C., Dell, A., and Albers, S.-V. (2011). Sulfoquinovose synthase – an important enzyme in the N-glycosylation pathway of *Sulfolobus acidocaldarius*. Mol. Microbiol. *82*, 1150–1163.

Peck, S.C., Denger, K., Burrichter, A., Irwin, S.M., Balskus, E.P., and Schleheck, D. (2019). A glycyl radical enzyme enables hydrogen sulfide production by the human intestinal bacterium *Bilophila wadsworthia*. Proc. Natl. Acad. Sci. U S A *116*, 3171–3176.

Schurmann, M., and Sprenger, G.A. (2001). Fructose-6-phosphate aldolase is a novel class I aldolase from *Escherichia coli* and is related to a novel group of bacterial transaldolases. J. Biol. Chem. *276*, 11055–11061.

Sharma, M., Abayakoon, P., Lingford, J.P., Epa, R., John, A., Jin, Y., Goddard-Borger, E.D., and Williams, S.J. (2020). Dynamic structural changes accompany the production of dihydroxypropanesulfonate by sulfolactaldehyde reductase. ACS Catal. *10*, 2826–2836.

Singh, S.B., and Lin, H.C. (2015). Hydrogen sulfide in physiology and diseases of the digestive tract. Microorganisms *3*, 866–889.

Speciale, G., Jin, Y., Davies, G.J., Williams, S.J., and Goddard-Borger, E.D. (2016). YihQ is a sulfoquinovosidase that cleaves sulfoquinovosyl diacylglyceride sulfolipids. Nat. Chem. Biol. *12*, 215–217.

Tsoi, R., Wu, F., Zhang, C., Bewick, S., Karig, D., and You, L. (2018). Metabolic division of labor in microbial systems. Proc. Natl. Acad. Sci. U S A *115*, 2526–2531.

Tyrrell, G.J., Turnbull, L., Teixeira, L.M., Lefebvre, J., Carvalho, M.d.G.S., Facklam, R.R., and Lovgren, M. (2002). *Enterococcus gilvus* sp. nov. and *Enterococcus pallens* sp. nov. isolated from human clinical specimens. J. Clin. Microbiol. *40*, 1140–1145.

iScience, Volume *23*

Supplemental Information

Environmental and Intestinal Phylum *Firmicutes* Bacteria Metabolize the Plant Sugar Sulfoquinovose via a 6-Deoxy-6-sulfofructose Transaldolase Pathway

Benjamin Frommeyer, Alexander W. Fiedler, Sebastian R. Oehler, Buck T. Hanson, Alexander Loy, Paolo Franchini, Dieter Spiteller, and David Schleheck

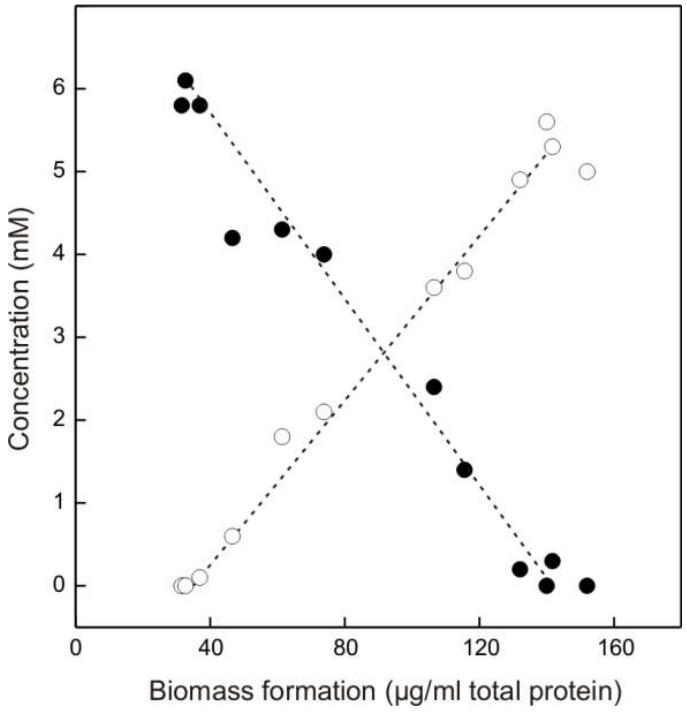

Figure S1. Linearized growth plot demonstrating complete substrate disappearance and stoichiometrical formation of 3-sulfolactate (SL) during growth of *B. aryabhattai* SOS1 with SQ, Related to Figure 1 and 6A. Concentrations of SQ (solid circles) and SL (open circles) were determined by HPLC at intervals during growth and the values plotted against biomass formation (total cellular protein). Data of one growth experiment (n=1) is shown.

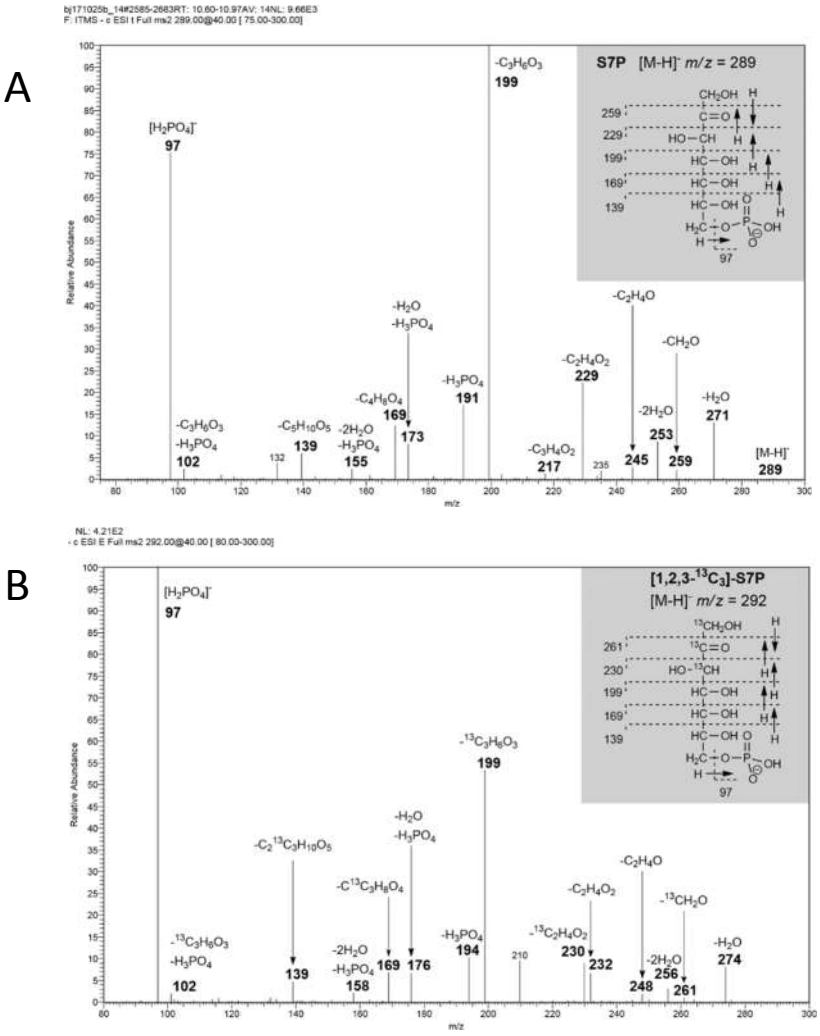

Figure S2. MS/MS fragmentation of unlabeled S7P analytical standard (A) and of [1,2,3-$^{13}C_3$]-S7P (B) as generated from $^{13}C_6$-SQ as substrate and unlabeled E4P as acceptor in cell extract of SQ-grown *B. aryabhattai* SOS1, Related to Figure 3. (**A**) Fragmentation pattern of the $[M-H]^-$ ions of unlabeled S7P standard. Fragmentation led to loss of one water (-18), formaldehyde (-30), two water (-36), ethanal (-44), $C_2H_4O_2$ (-60), $C_3H_4O_2$ (-72), dihydroxyacetone (-90), phosphoric acid (-98), phosphoric acid and water (-116), tetrose (-120), phosphoric acid and two water (-134), pentose (-150), and dihydroxyacetone and phosphate (-187) and the formation of phosphate (97). (**B**) Fragmentation pattern of the $[M-H]^-$ ions of [1,2,3-$^{13}C_3$]-S7P, as generated in enzyme reactions (see main text, **Figures 3, 4**), including corresponding mass shifts relative to that of the analytical standard (**A**) (271 → 274, 259 → 261, 253 → 256, 245 → 248, and 229 → 232/230), confirming a transfer of a $^{13}C_3$-glycerone moiety from $^{13}C_6$-SQ to unlabeled E4P concomitantly with formation of $^{13}C_3$-SLA (see **Figures 3** and **S6**).

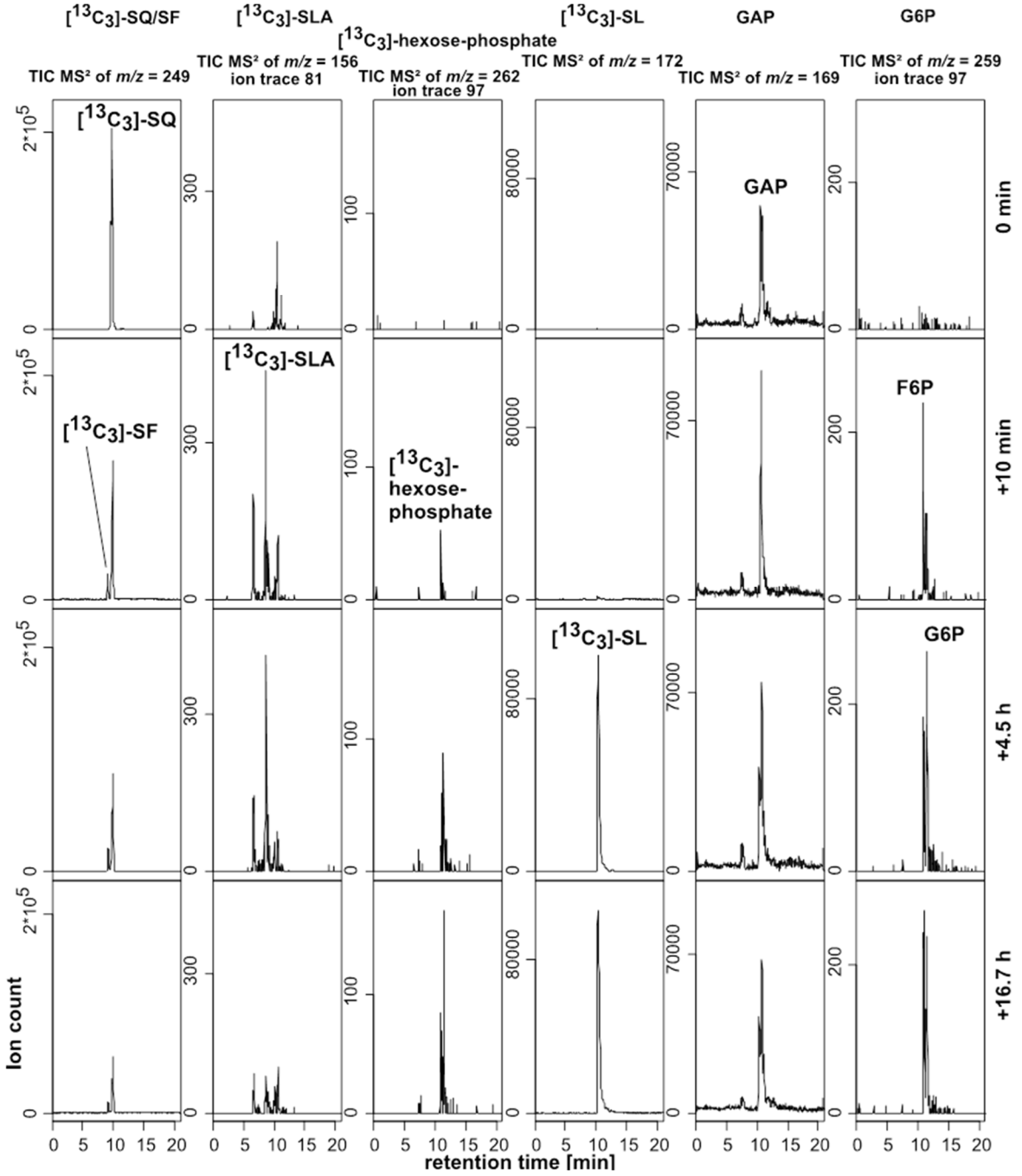

Figure S3. HPLC mass spectrometry confirming a transaldolase reaction in cell extracts of *B. aryabhattai* SOS1 using fully $^{13}C_6$-SQ as substrate and GAP as acceptor molecule, Related to Figure 3. The chromatograms illustrate conversion of $^{13}C_6$-SQ in the presence of GAP by cell extract of SQ-grown *Bacillus aryabhattai* SOS1, to $^{13}C_3$-SLA, which was further oxidized to $^{13}C_3$-SL, and to [$^{13}C_3$]-hexose phosphate. The reaction contained 50 mM $(NH_4)_2CO_3$ (pH 9.0), 1 mM DTT, 1 mM $MnCl_2$, 0.5 mM $MgCl_2$, 2 mM $^{13}C_6$-SQ, 6 mM NAD^+ and 6 mM GAP. Samples were taken and analyzed directly before addition of extract and after 10 min, 4.7

h and 21.4 h. For the organosulfonates, the total-ion chromatograms (TICs) recorded in the negative ion mode from the MS/MS fragmentation of the $[M-H]^-$ ions are shown. For SLA, the MS/MS-ion trace of the fragment from loss of the sulfonate group (*m/z* = 81) is shown. The $[^{13}C_3]$-hexose-phosphates were detected *via* fragmentation of $[M-H]^-$ ion (*m/z* = 262) and recording the phosphate-specific fragment *m/z* = 97. Note that F6P and G6P eluted in two peaks with very similar same retention time (**Figure S12**). Triose phosphates were detected by the $[M-H]^-$ ion trace (*m/z* = 169). Formation of unlabeled F6P and G6P can be explained by enzymes active in the cell extract for gluconeogenesis, e.g. through conversion of the added GAP.

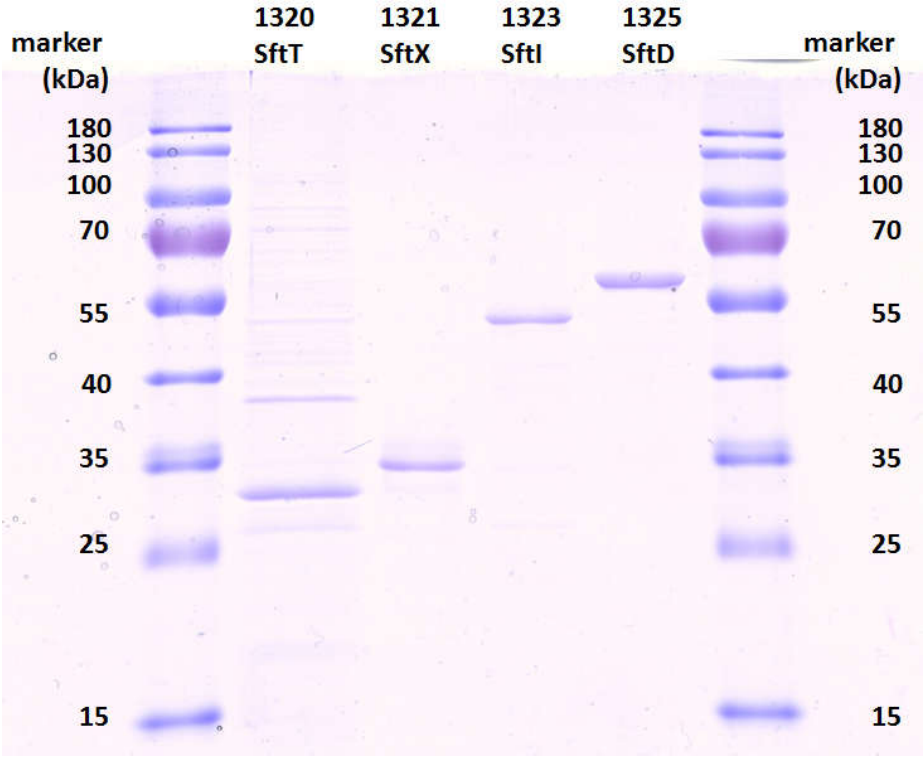

Figure S4. SDS-PAGE of purified recombinant proteins, Related to Figure 4. Protein standards, lane 1 and 6; *B. aryabhattai* SftT (25.3 + 4.1 [His-tag] kDa), lane 2; SftX (25,6 + 4.1 kDa), lane 3; SftI (49.7 + 4.1 kDa), lane 4; and SftD (52.1 + 4.1 kDa), lane 5. Note that we expressed and purified also domain-of-unknown-function (DUF4867) protein SftX, but could not attribute any activity to this protein, e.g., when tested individually or combination with SftITD.

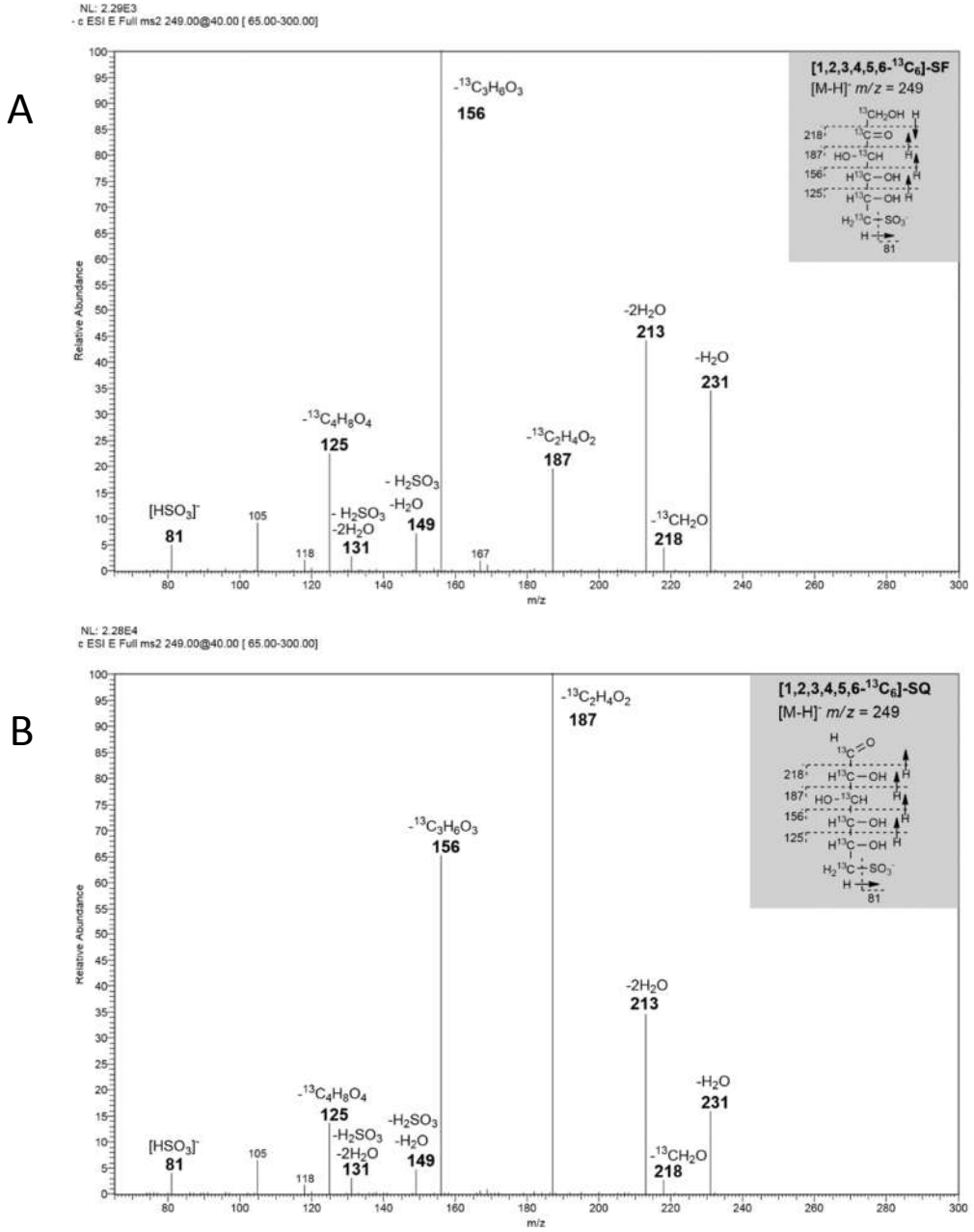

Figure S5. MS/MS fragmentation of $^{13}C_6$-SF (A) and $^{13}C_6$-SQ (B), Related to Figures 3 and 4. (A) Fragmentation of the $[M-H]^-$ ions of the $^{13}C_6$-SF (**Figures 3, 4**) led to a pattern as observed for unlabeled SF (**Denger et al., 2014**) including corresponding mass shifts (225 → 231, 213 → 218, 207 → 213, 183 → 187, 153 → 156, 143 → 149, 125 → 131, and 123 →125). (B) Fragmentation of the $[M-H]^-$ ions of $^{13}C_6$-SQ led to a pattern as for unlabeled SQ (**Denger et al., 2014**) including corresponding mass shifts (225 → 231, 213 → 218, 207 → 213, 183 → 187, 153 → 156, 143 → 149, 125 → 131, and 123 →125).

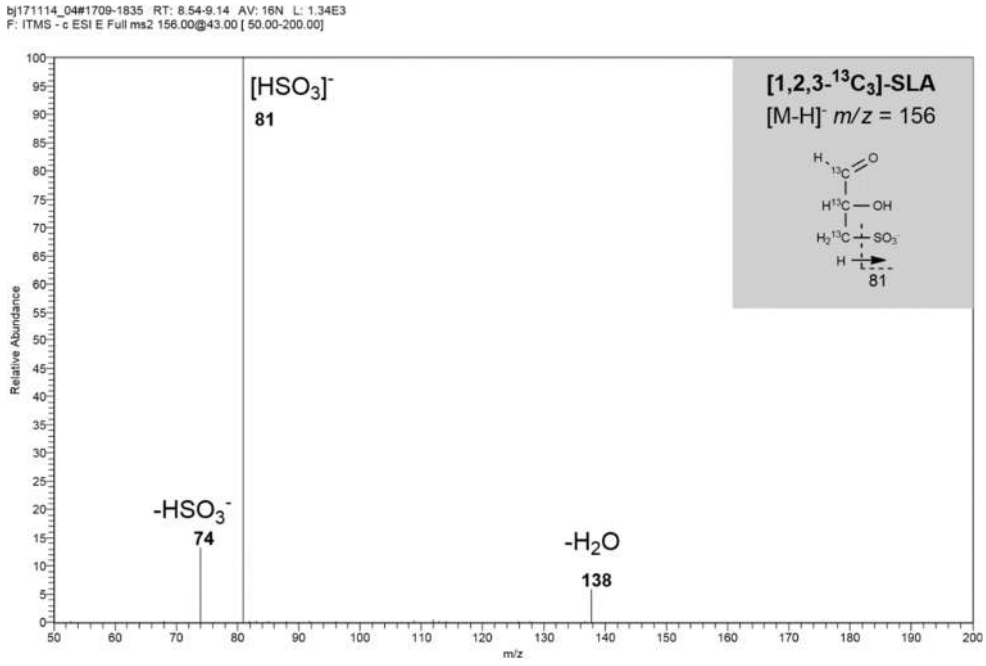

Figure S6. MS/MS fragmentation of $^{13}C_3$-SLA, Related to Figures 3 and 4. Fragmentation of the [M-H]$^-$ ions of the [1,2,3-$^{13}C_3$]-SLA (**Figures 3, 4**) led to a pattern as published previously (**Felux et al., 2015**) but with corresponding mass shifts (135 → 138, 71 → 74).

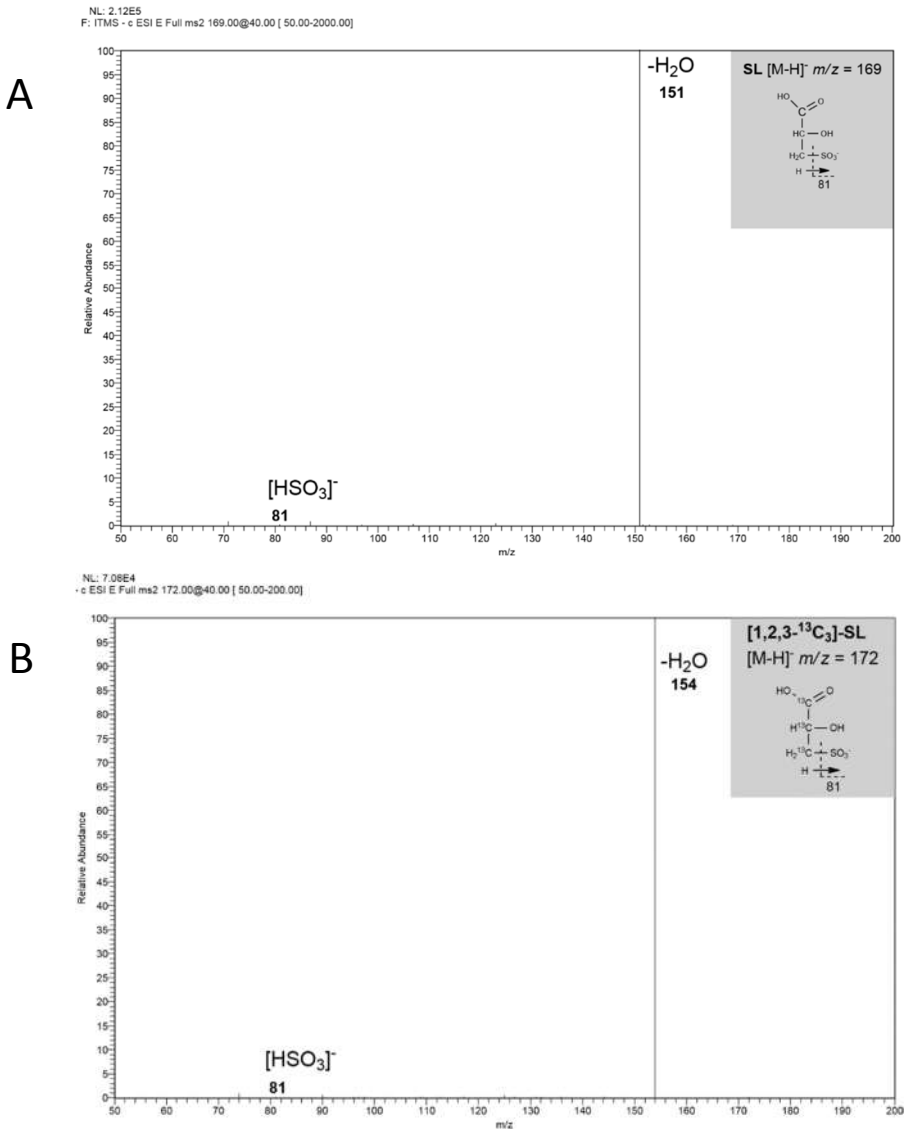

Figure S7. MS/MS fragmentation of $^{13}C_3$-SL, Related to Figures 3 and 4. (**A**) Fragmentation of the [M-H]$^-$ ions of authentic SL standard. Ion intensities were different than previously published (**Felux et al., 2015**) because of a stronger collision-induced dissociation energy was used. (**B**) Fragmentation of the [M-H]$^-$ ions of the [1,2,3-$^{13}C_3$]-SL (**Figures 3, 4**) including corresponding mass shift (151 → 154) of the major fragment.

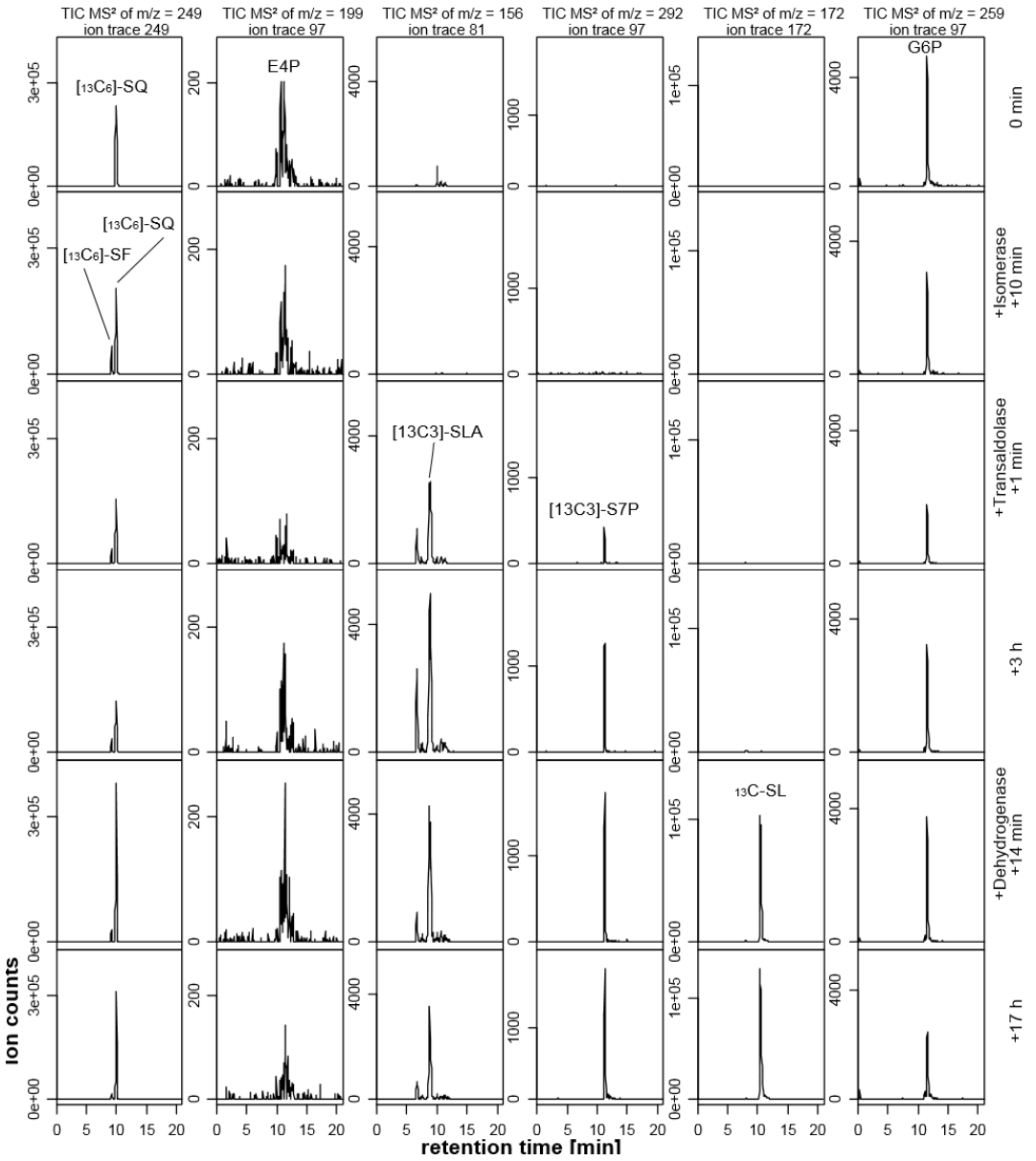

Figure S8. *In-vitro* reconstitution of the SFT pathway by recombinant enzymes using E4P as acceptor instead of GAP, Related to Figure 4. Cleavage of $^{13}C_6$-SQ *via* $^{13}C_6$-SF to [1,2,3-$^{13}C_3$]-S7P and $^{13}C_3$-SLA in the presence of unlabeled E4P, and oxidation of the $^{13}C_3$-SLA to $^{13}C_3$-SL in the presence of NAD^+. The reaction mixture initially contained 2 mM $^{13}C_6$-SQ and 6 mM E4P (0 min); note that purchased E4P contained impurities of G6P. SQ isomerase SftI (200 µg/ml) was added and the reaction sampled after 10 min. Then, SF transaldolase SftT (100 µg/ml) was added and the reaction sampled after 3 h. Finally, SLA-dehydrogenase SftD was added (200 µg/ml) and NAD^+ (6 mM) and the reaction sampled after 14 min and 17 h. Note that even after 17 h reaction time, substrate conversion was incomplete because of the promiscuous activity of SftD oxidizing E4P in the presence of NAD^+.

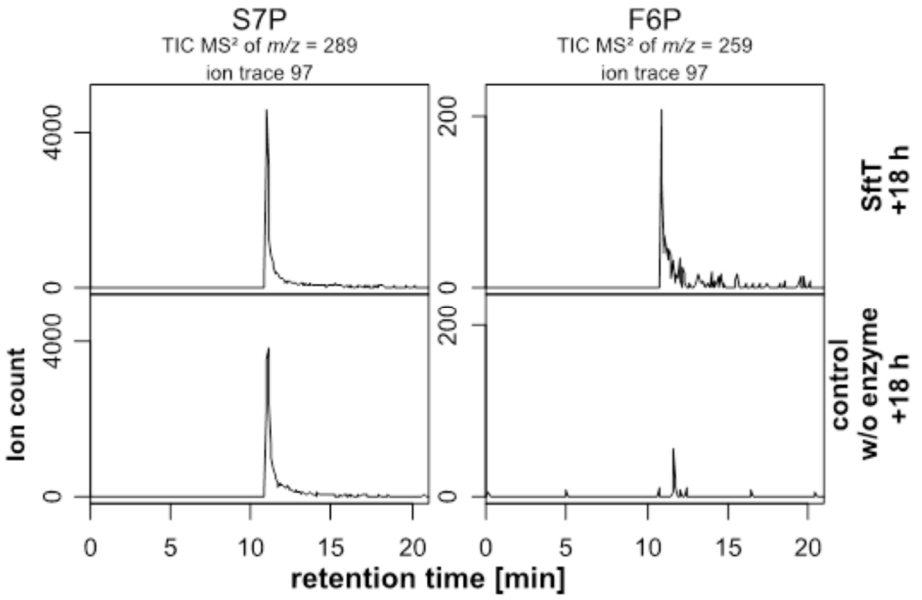

Figure S9. Promiscuous activity of transaldolase SftT as S7P transaldolase in the presence of GAP as acceptor, Related to Figure 4. HPLC MS/MS-ion traces demonstrating conversion of S7P (left panel) to F6P (right panel) in the presence of GAP and transaldolase SftT (100 µg/ml), in comparison to a control reaction containing GAP but not SftT. The reaction mixture initially contained 1 mM S7P, 1 mM GAP, 50 mM $(NH_4)_2CO_3$ (pH 9.0), 1 mM DTT, 1 mM $MnCl_2$ and 1 mM $MgCl_2$. Note that the purchased GAP contained impurities of F6P (as visible for the control reaction).

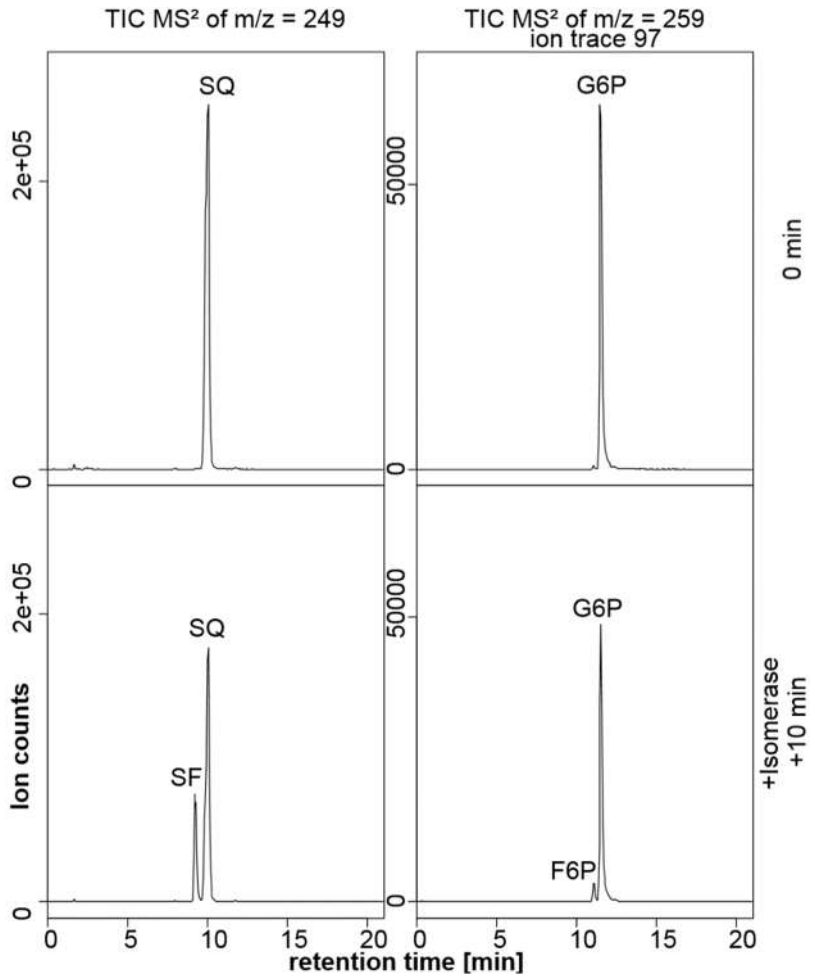

Figure S10. Promiscuous activity of isomerase SftI as G6P isomerase, Related to Figure 4. HPLC-MS chromatograms demonstrating conversion of SQ to SF (left panel) and of G6P to F6P (right panel) by isomerase SftI. The reaction mixture initially contained 2 mM SQ or 6 mM G6P, and 50 mM $(NH_4)_2CO_3$ (pH 9.0), 1 mM DTT, 1 mM $MnCl_2$ and 1 mM $MgCl_2$. Samples were taken before and 10 min after addition of enzyme (100 μg/ml).

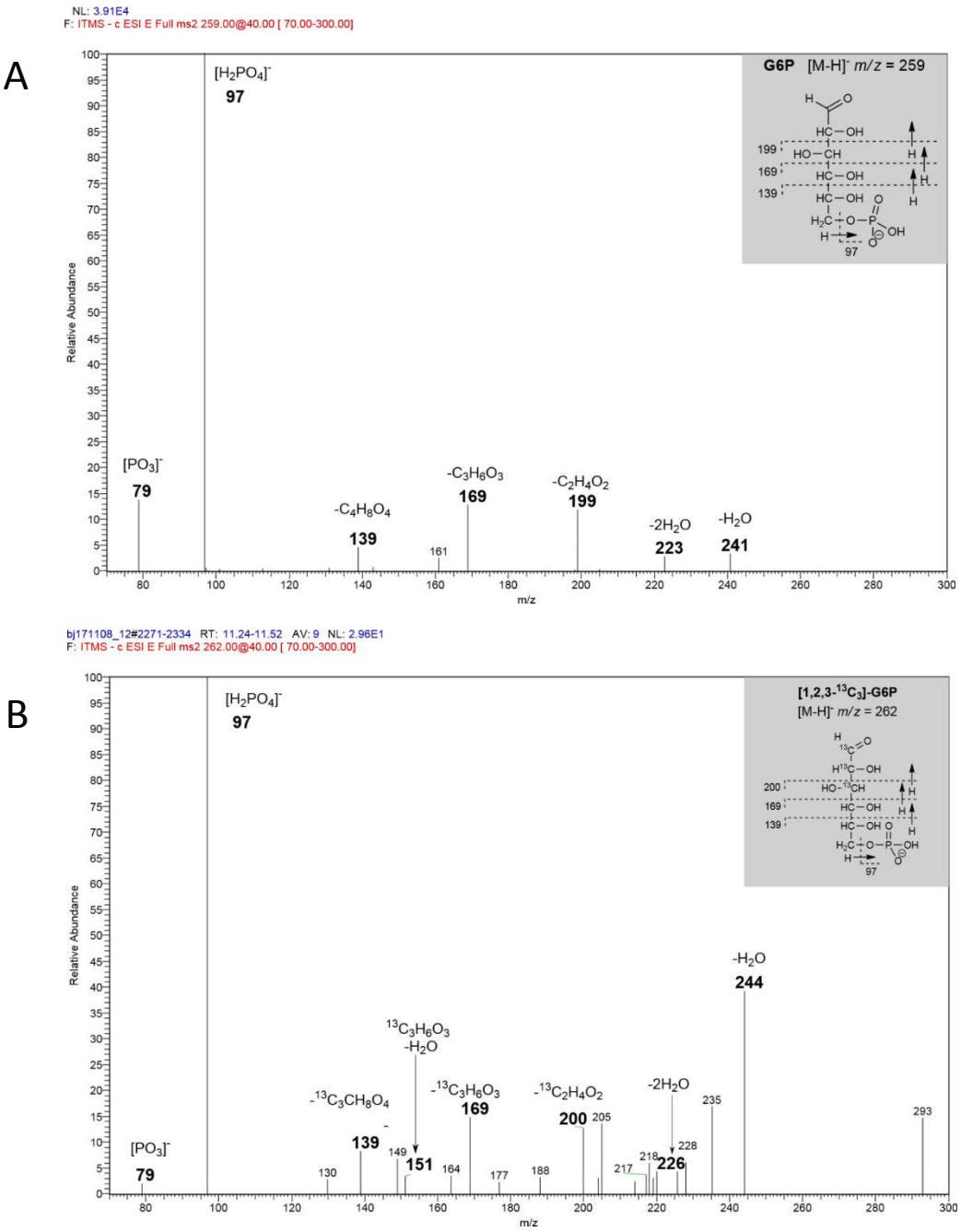

Figure S11. MS/MS fragmentation of G6P (A) and [1,2,3-$^{13}C_3$]-G6P (B), Related to Figure 4. (**A**) Fragmentation of the $[M-H]^-$ ions of G6P led to a loss of water (-18), two water (-36), $C_2H_4O_2$ (-60), triose (-90), tetrose (-120), and the formation of phosphate characteristic peaks 97 and 79 (**de Souza et al., 2009**). (**B**) Fragmentation pattern of the $[M-H]^-$ ions of [1,2,3-$^{13}C_3$]-G6P inclusive corresponding mass shifts (241 → 244, 223 → 226, and 199 → 200). Note that the fragmentation patterns for F6P and G6P are very similar, but that F6P eluted earlier than G6P in HPLC (**Figure S10**).

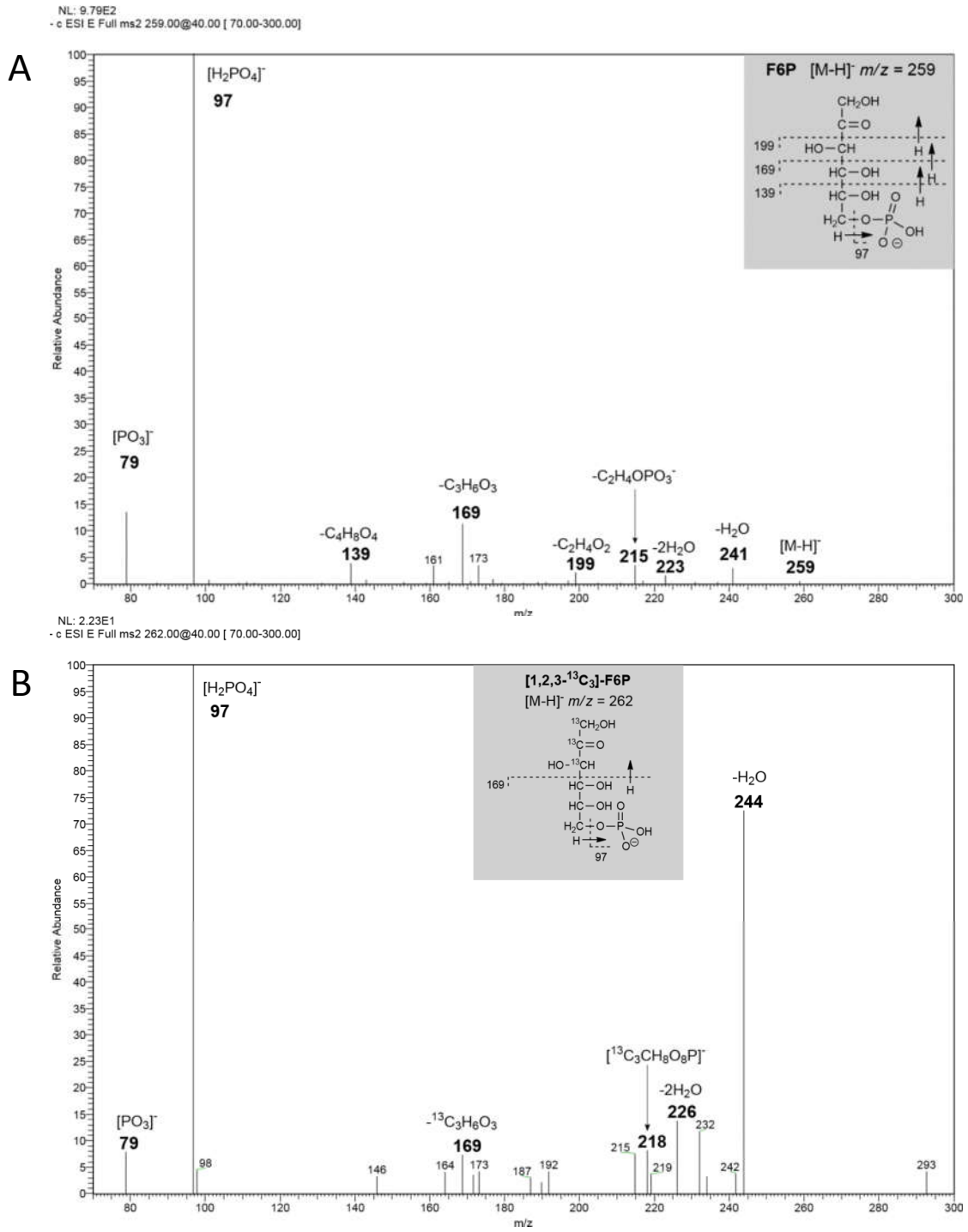

Figure S12. MS/MS fragmentation of F6P (A) and [1,2,3-$^{13}C_3$]-F6P (B), Related to Figure 4. (**A**) Fragmentation of the $[M-H]^-$ ions of F6P led to a loss of water (-18), two water (-36), $C_2H_4O_2$ (-60), triose (-90), tetrose (-120), and the formation of phosphate characteristic peaks 97 and 79 (**de Souza et al., 2009**). (**B**) Fragmentation of the $[M-H]^-$ ions of [1,2,3-$^{13}C_3$]-F6P inclusive corresponding mass shifts (241 → 244; 223 → 226 and 199 → 200). Note that the fragmentation for F6P and G6P is very similar, but that F6P eluted earlier than G6P in HPLC (**Figure S10**).

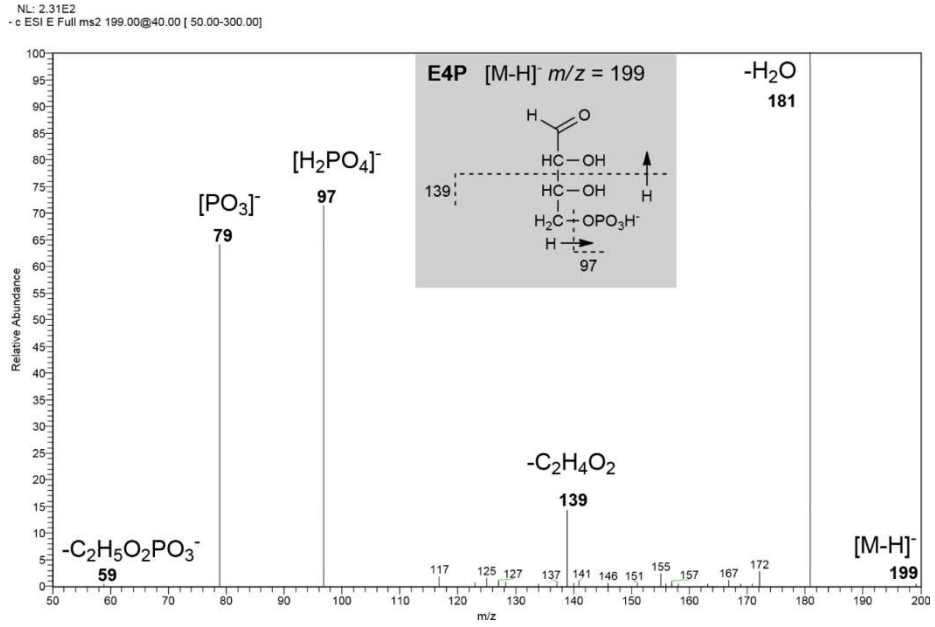

Figure S13. MS/MS fragmentation of E4P parental ion [M-H]$^-$, Related to Figure 3. Fragmentation led to a loss of water (-18), $C_2H_4O_2$ (-30), and the formation of characteristic phosphate peaks 97 and 79 (**de Souza et al., 2009**).

Table S1. Related to Figures 2 and 4. Primer sequences (5'-3') for directional cloning of *Bacillus aryabhattai* SOS1 pathway genes, plasmid-insert sequencing and 16S-rRNA gene sequencing.

1320_for3*	CACCATGAAGTATTTTTTAGATAGTGCCATTTTAGAG
1320_rev2	AAGCCCCTCAAAGAAGATAATAAGATTC
1321_for3*	CACCATGGGCAGCTTTCAATACATGAAAGACTT
1321_rev1	AGTAGAACTACGCCGTTAAGAGCAACTT
1322_for1*	CACCATGTCAGGTACCTTAAACGTAACTAAAGGG
1322_rev2	ATACTAATTTTCCGCTTGACTACACTTCTTAT
1323_for2*	CACCATGCAAAATACGACAGTTTTATATGTGC
1323_rev1	TTGTATCTTTCATGTTCTCAAACTCCTT
1325_for4*	CACCATGACGAGTTTAACTCAAGTCAAACAATATG
1325_rev1	AAAAATCCCGAAAATAGGAAGAAGGA
T7 forward	TAATACGACTCACTATAGGG
T7 reverse	TAGTTATTGCTCAGCGGTGG
8F	AGAGTTTGATYMTGGCTC
1492R	GGYTACCTTGTTACGACTT

*Adaptor sequence for directional cloning underlined

TRANSPARENT METHODS

Enzyme nomenclature. We suggest that *B. aryabhattai* SQ isomerase SftI would belong to NC-IUBMB (Nomenclature Commission of the International Union of Biochemistry and Molecular Biology) subgroup EC 5.3.1., with the name sulfoquinovose isomerase (systematic name 6-deoxy-6-sulfoglucose aldose-ketose-isomerase); it showed activity also as D-glucose 6-phosphate isomerase (EC 5.3.1; D-glucose 6-phosphate aldose-ketose-isomerase). SF transaldolase SftT would belong to EC 2.2.1.2 with the name sulfofructose transaldolase (systematic name 6-deoxy-6-sulfofructose:D-glyceraldehyde-3-phosphate glycerone-transferase); it showed activity also as sedoheptulose-7-phosphate transaldolase (EC 2.2.1.2; sedoheptulose-7-phosphate:D-glyceraldehyde-3-phosphate glyceronetransferase). SLA dehydrogenase SftD belongs to the EC 1.2.1 with the name sulfolactaldehyde dehydrogenase (systematic name 3-sulfolactaldehyde:NAD^+ oxidoreductase); it showed activity also as erythrose-4-phosphate and glyceraldehyde-3-phosphate:NAD^+ oxidoreductase.

Chemicals. NAD^+, fructose-6-phosphate disodium salt, D/L-gyceraldehyde-3-phosphate (45-55 mg/ml in H_2O solution), glucose-6-phosphate sodium salt and chloramphenicol were supplied by Sigma (now Merck KGaA, Darmstadt Germany), and D-erythrose-4-phosphate sodium salt by Sigma, Carbosynth (Compton, UK) and Santa Cruz Biotechnology (Dallas, Texas). D-sedoheptulose-7-phosphate barium salt was from Carbosynth. SQ, $^{13}C_6$-SQ and SL were synthesized by MCAT GmbH (Donaueschingen, Germany). DHPS was synthesized and validated by NMR as reported previously (**Mayer et al., 2010; Denger et al., 2012**). 1,4-Dithiothreitol was supplied by Carl Roth (Karlsruhe, Germany) (p.a. grade) and VWR International GmbH (Electran molecular biology grade). Adenosin-5'-triphosphate disodium salt was from Serva (Heidelberg, Germany), manganese(II) chloride tetrahydrate (p. a. grade) from Riedel-de Haën (now Honeywell, Seelze, Germany). Ampicillin was purchased from Carl

Roth (Karlsruhe, Germany), isopropyl-β-D-thiogalactopyranosid (IPTG) from carbolution chemicals GmbH (St. Ingbert, Germany), and Imidazol from Merck (Kenilworth, New Jersey, US). Gases for anaerobic cultivation were purchased from Messer-Griesheim (Darmstadt, Germany) and Sauerstoffwerke Friedrichshafen (Friedrichshafen, Germany).

Enrichment, isolation and identification of *Bacillus aryabhattai* SOS1. *B. aryabhattai* SOS1 (DSM 104036) was isolated from an enrichment cultures using a maple leaf as inoculum (collected in the forest of the campus of University of Konstanz), and by using the following purification strategy. Sterile phosphate-buffered (pH 7.2) mineral salts medium (**Thurnheer et al., 1986**) (5 ml) with 6 mM SQ as sole carbon and energy source in 30 ml glass tubes (Corning, USA) was used to wash microorganisms off the leaf by vortexing. The leaf was removed and the enrichment culture incubation at 30°C shaking at 165 rpm. For enrichment and isolation of the other SQ-degrading strains, as mentioned in the results section, the inocula were prepared as follows. Samples of different soils (forest or agricultural soils, collected at around University of Konstanz; approx. 1 g) were suspended in sterile mineral-salts medium (10 ml) and sonified (30 s) to detach microorganisms; supernatant of these soil suspensions were used as inoculum (100 µl). Heat-treated (pasteurized) soil inocula were prepared when the soil samples were dried for three days at 40°C. Appr. 50 mg were added to SQ minerals-salts medium, and these inoculated cultures were heated at 65°C or 80°C for 1 h prior to incubation at 30°C, 165 rpm shaking. A water sample from a pond (collected at around University of Konstanz) was used as inoculum (100 µl) when added directly to the culture tube without heat treatment. When growth was visible as turbidity and by presence of bacteria (microscopy), and after SQ disappearance was confirmed by HPLC analysis, 5 - 15 µl of the outgrown cultures were transferred into fresh, sterile 3 ml SQ mineral-salts medium in 30-ml glass tubes. Sub-cultivations were pursued until to the 5th transfer, after which samples of culture fluid were streaked on LB5 plates (10 g/l tryptone, 5 g/l yeast extract, 5 g/l NaCl, 15 g/l agar); the plates were incubated at 30°C in the dark. From these plates, each colony type was picked individually and transferred back into

liquid cultures with SQ-salts medium. This procedure was repeated until a homogeneous colony picture on LB plates was obtained. The isolates were identified by sequencing of the 16S rRNA gene (primers 8F and 1492R; **Table S1**) through colony PCR. Sanger sequencing was performed on purified amplicons (Eurofins, Germany) and characterized against the NCBI and RDP databases.

***B. aryabhattai* SOS1 cultivation and preparation of cell extracts.** Strain SOS1 was grown at 30°C, 150-180 rpm shaking, in the range from 5 ml culture medium in 30-ml glass tubes up to 2 liters in Erlenmeyer flasks, using the mineral salts medium described above with either SQ (6 or 12 mM) or glucose (3 or 6 mM) as substrate; concentrations were adjusted to compensate for half the molar growth yield with SQ *vs.* glucose. Cultures were inoculated with a colony from LB5-agar plates (5-ml scale) or with 0.5-5% (v/v) of outgrown pre-culture. Growth was monitored as optical density at 580 nm (OD580) either directly in the glass tubes or through side-arm flasks in a tube photometers (model M 107; Campspec), or in samples of 1 ml culture fluid in cuvettes (Novaspec Plus; Amersham Biosciences). For determination of substrate disappearance and product formation by HPLC (see below), samples from the supernatant obtained after centrifugation (10 minutes, 16,100 x g, 20°C) of 1 ml of culture fluid were taken; the cell pellet was retained for total protein determination by Lowry assay (**Kennedy and Fewson 1968**) against bovine serum albumin (BSA) as a standard. For proteomic analysis and preparation of cell extracts, cells were grown in larger scales in Erlenmeyer flasks and harvested by centrifugation (15 min, 15,000 x g, 10°C). The cell pellets were stored frozen (-20°C).

For two-dimensional (2D) protein gel electrophoresis and total proteomics, cell pellets were re-suspended in Tris-HCl buffer (pH 7.5) containing 25 µg/ml DNAse and 2 mM $MgCl_2$. The cells were disrupted by five passages through a chilled French Pressure Cell (SLM Instruments, USA) at 140 MPa and unbroken cells and debris was removed by centrifugation (10 min, 15,000 x g, 4°C) to obtain cell extracts. Samples of cell extract were submitted to total proteomic

analysis (see below). For 2D-protein gel electrophoresis, membrane fragments were removed by ultracentrifugation (1 h, 70,000 x g, 4°C; Beckman Optima TL) to obtain soluble protein fraction, which was desalted using PD-10 columns (GE Healthcare) prior to 2D-protein gel electrophoresis (see below). Protein concentrations in the extracts were determined through Bradford assay (**Bradford 1976**) against BSA as standard.

For enzyme assays, the cell pellets were resuspended and washed twice with $(NH_4)_2CO_3$ buffer (50 mM, pH 9.0) by centrifugation (15 min, 5000 x g, 4°C); after the washing, 1 U/ml DNase was added. The lysis was performed by five passages through a chilled French pressure cell at 140 MPa. Cell debris was removed by centrifugation (15 min, 21.380 x g, 4°C) and small molecules were removed by gel filtration if appropriate (exclusion size 1-5 kDa; illustra NAP-10 gel filtration columns, GE Healthcare Life Sciences).

Draft-genome sequencing and proteomic analysis of *B. aryabhattai* SOS1. Genomic DNA of strain SOS1 was prepared by the CTAB-protocol (**William et al., 2012**) including RNase treatment. Whole genome shotgun sequencing of strain SOS1 was performed by GATC Biotech (Konstanz, Germany; now Eurofins) using an Illumina HiSeq 2500 platform and a 2x125bp paired-end library, which generated 11,92 million reads. The program Trimmomatic v0.33 (**Bolger et al., 2014**) was used to remove adapters and filter the reads by quality with default settings, as well as to discard sequences shorter than 50 nucleotides. The filtered reads were assembled *de novo* using the program SOAPdenovo v2.04 (**Luo et al., 2012**) with a k-mer size of 67 and setting the minimum contig length at 200 bp. The *de novo* assembly procedure resulted in 383 sequences (N50: 0.808 Mb) that were further scaffolded by the reference-guided algorithm implemented in Ragout 2.0b (**Kolmogorov et al., 2014**) using the genome of *Bacillus aryabhattai* T61 as reference. The final assembly of *B. aryabhattai* SOS1 included 359 sequences (N50: 4.638 Mb).

2D-protein gel electrophoresis (isoelectric focusing and SDS gel electrophoresis) of the soluble protein fraction of strain SOS1 was conducted as described previously (**Felux et al., 2015**). Total proteomics of cell extracts, and identification of proteins in spots excised from the SDS gels, was done as described previously (**Denger et al., 2014; Felux et al., 2015**, **Schmidt et al., 2013**) at the Proteomics Centre of the University of Konstanz (https://www.biologie.uni-konstanz.de/proteomics-centre/) with the exception that each sample was analyzed twice on a Orbitrap Fusion with EASY-nLC 1200 (Thermo Fisher Scientific), and tandem mass spectra were searched against the protein database using Mascot (Matrix Science) and Proteom Discoverer V1.3 (Thermo Fisher Scientific) with "Trypsin" enzyme cleavage, static cysteine alkylation by chloroacetamide, and variable methionine oxidation (**Peck et al., 2019**).

HPLC for determination of substrate and product concentrations in cultures. SQ, DHPS and SL in samples of culture supernatant (see above) were separated by hydrophilic interaction chromatography (HILIC) using an HPLC apparatus (Prominence LC-20A System; Shimadzu), and were detected by an Evaporative Light Scattering Detector (ELSD) (model ZAM 3000; Schambeck SFD GmbH, Germany). A SeQuant ZIC-HILIC HPLC Column (Merck, Germany) as described previously (**Denger et al., 2014**) was used for the separation. Samples of culture supernatants (0.6 ml) were mixed with acetonitrile (0.3 ml) in HPLC-vials. The injection volume was 10 µl. The column temperature was set at 30°C. The eluents were (A) 0.1 M ammonium acetate in water supplemented with 10% acetonitrile, and (B) 100% acetonitrile. The flow rate was 0.75 ml/min. The HPLC gradient was set from 90% B to 65% B in 25 min; hold at 65% B for 10 min; gradient to 90% B in 0.5 min; hold (reequilibration) at 90% B for 9.5 min. SQ, DHPS and SL were identified by their specific retention time against authentic standards (SQ, 25.9 - 26.4 min; DHPS, 17.6 - 17.7 min; SL, 27.2 - 27.6 min) and quantified by peak area integration against authentic standards (see above). SL was quantified also by ion chromatography with suppression under conditions described previously (**Styp von Rekowski et al., 2005**); SL eluted after 6.1 min.

HPLC-MS of substrate turnover in *B. aryabhattai* SOS1 cell extracts and in reactions with recombinant enzymes. HPLC-MS/MS measurements were conducted with a Finnigan Surveyor Autosampler Plus and MS Pump Plus coupled with a Finnigan LTQ (Thermo Fisher Scentific). The SeQuant ZIC-HILIC column (see above) was used for the separation fitted with an upstream prefilter (HICHROM HI-704 with 2 µm frit) and precolumn (ZIC HILIC Guard SeQuant, Merck). Solvent A was 0.1 M ammonium acetate in milliQ H_2O or double distilled H_2O with 10 % acetonitrile. Solvent B was acetonitrile with 0.1% glacial acetic acid. The flow rate was 0.3 ml/min. The HPLC gradient program started at 90% solvent B, decreasing to 10% B over 20 min, increasing back to 90% B within 1 min and equilibrating on 90% B for 5 min. The compounds were ionized by negative electrospray ionization (ESI). MS chromatograms and fragmentation patterns were analyzed with Xcalibur 2.0 (Thermo Fisher Scientific). Multiple plot figures were created by using the raw data exported from Qual browser 2.0 *via* .csv-files into Excel 2010 (Microsoft Corporation). These files were used by a custom written r-studio (Version 1.0.143; RStudio, Inc.) script to generate the figures.

The retention times of the substances separated by the HPLC gradient program and the ESI-MS/MS fragmentation patterns of the observed analytes were as follows: [1,2,3,4,5,6-$^{13}C_6$]-SQ retention time 9.8 min; [1,2,3,4,5,6-$^{13}C_6$]-SQ ESI-MS *m/z* (% base-peak): $[M-H]^-$ 249 (100); [1,2,3,4,5,6-$^{13}C_6$]-SQ ESI-MS/MS of $[M-H]^-$ 249: 231 (16), 218 (3), 213 (35), 187 (100), 156 (65), 149 (5), 131 (3), 125 (14), 81 (4). [1,2,3,4,5,6-$^{13}C_6$]-SF retention time 9.3 min; [1,2,3,4,5,6-$^{13}C_6$]-SF ESI-MS *m/z* (% base-peak) $[M-H]^-$ 249 (100); [1,2,3,4,5,6-$^{13}C_6$]-SF ESI-MS/MS of $[M-H]^-$ 249: 231 (33), 218 (4), 213 (43), 187 (20), 156 (100), 149 (7), 131 (3), 125 (23), 81 (5). [1,2,3-$^{13}C_3$]-SLA retention time 8.8 min. [1,2,3-$^{13}C_3$]-SLA ESI-MS *m/z* (% base-peak) $[M-H]^-$ 249 (100); [1,2,3-$^{13}C_3$]-SLA ESI-MS/MS of $[M-H]^-$ 156: 138 (6), 81 (100), 74 (13). SL retention time 10.5; SL ESI-MS *m/z* (% base peak) $[M-H]^-$ 169 (100); SL ESI-MS/MS of $[M-H]^-$ 169: 151 (100), 81 (<1). [1,2,3-$^{13}C_3$]-SL retention time 10.5; [1,2,3-$^{13}C_3$]-SL ESI-MS *m/z* (% base peak) $[M-H]^-$ 169 (100); [1,2,3-$^{13}C_3$]-SL ESI-MS/MS of $[M-H]^-$ 172: 154 (100),

81 (>1). GAP retention time 12.5; GAP ESI-MS *m/z* (% base peak) $[M-H]^-$ 169 (100); GAP ESI-MS/MS of $[M-H]^-$ 169: 151 (21), 141 (7), 97 (100), 79 (32). E4P retention time 10.6; E4P ESI-MS *m/z* (% base peak) $[M-H]^-$ 199 (100); E4P ESI-MS/MS of $[M-H]^-$ 199: 199 (<1), 181 (100), 139 (14), 97 (71), 79 (64). S7P retention time 11.2; S7P ESI-MS *m/z* (% base peak) $[M-H]^-$ 289 (100); S7P ESI-MS/MS $[M-H]^-$ 289: 289 (<1), 271 (13), 259 (2), 253 (8), 245 (2), 229 (22), 217 (1), 199 (100), 191 (17), 173 (8), 169 (13), 155 (2), 139 (6), 102 (3), 97 (75). [1,2,3-$^{13}C_3$]-S7P retention time 11.2; [1,2,3-$^{13}C_3$]-S7P ESI-MS *m/z* (% base peak) $[M-H]^-$ 292 (100); [1,2,3-$^{13}C_3$]-S7P ESI-MS/MS $[M-H]^-$ 292: 274 (8), 261 (1), 256 (3), 248 (2), 232 (7), 230 (9), 199 (53), 194 (10), 176 (7), 169 (7), 158 (2), 139 (5), 102 (1), 97 (100). G6P retention time 11.5; G6P ESI-MS *m/z* (% base peak) $[M-H]^-$ 259 (100); G6P ESI-MS/MS $[M-H]^-$ 259: 241 (3), 223 (3), 199 (12), 169 (13), 139 (5), 97 (100), 79 (14). [1,2,3-$^{13}C_3$]-G6P retention time 11.5; [1,2,3-$^{13}C_3$]-G6P ESI-MS *m/z* (% base peak) $[M-H]^-$ 262 (100); [1,2,3-$^{13}C_3$]-G6P ESI-MS/MS $[M-H]^-$ 262: 244 (2), 226 (1), 200 (4), 169 (12), 139 (4), 97 (100), 79 (13). F6P retention time 11.0; F6P ESI-MS *m/z* (% base peak) $[M-H]^-$ 259 (100); F6P ESI-MS/MS $[M-H]^-$ 259: 241 (3), 223 (1), 199 (2), 169 (11), 139 (4), 97 (100), 79 (14). [1,2,3-$^{13}C_3$]-F6P retention time 11.0; [1,2,3-$^{13}C_3$]-F6P ESI-MS *m/z* (% base peak) $[M-H]^-$ 262 (100); [1,2,3-$^{13}C_3$]-F6P ESI-MS/MS $[M-H]^-$ 262: 244 (8), 226 (4), 200 (4), 169 (11), 139 (3), 97 (100), 79 (8).

Enzyme assays in cell extracts. For screening of formation of sulfo-EMP or sulfo-ED pathway intermediates in cell extracts of strain SOS1, Tris-HCl buffer (50 mM, pH 7.8) or potassium phosphate buffer (50 mM, pH 6.5) containing 200 µg/ml soluble protein fraction, 2 mM SQ, 4 mM NAD^+, 4 mM $NADP^+$, 8 mM ATP and 0.5 mM Mg^{2+} was incubated at room temperature. At intervals, samples (150 µl) of the enzyme assay were transferred to dichloromethane (50 µl) and vortexed for 3 s, in order to stop enzymatic activity, and centrifuged (15 min, 21.380 x g, 4°C); 100 µl of the upper aqueous phase was transferred into HPLC vials. Substrate disappearance and product formation was analyzed *via* HPLC-MS (see above) but with additional screening for the ions of sulfo-EMP or sulfo-ED pathway intermediates (**Denger et**

al., 2014): *m/z* $[M-H]^-$ of 241 for sulfogluconolactone and 2-keto-3,6-dideoxy-6-sulfogluconate, 256 for 6-deoxy-6-sulfogluconate and 323 for 6-deoxy-6-sulfofructose-1-phosphate.

For enzymatic assays with the SFT pathway enzymes in cell extracts of strain SOS1, the $(NH_4)_2CO_3$ buffered cell extract or gel-filtered cell extract (see above) was used (0.1 mg/ml protein) and incubated in 50 mM $(NH_4)_2CO_3$ buffer (pH 9.0) containing 1 mM 1,4-dithiothreitol (DTT), 1 mM $MnCl_2$, 0.5 mM $MgCl_2$, 6 mM SQ or $^{13}C_6$-SQ, 4 mM NAD^+ and optionally 6 mM erythrose-4-phosphate or 6 mM glyceraldehyde-3-phosphate as acceptor. Samples (150 µl) for HPLC-MS analysis were taken at intervals and transferred to dichloromethane (50 µl) and vortexed for 3 s, in order to stop enzymatic activity, and centrifuged (15 min, 21.380 x g, 4°C); 100 µl from the aqueous phase was transferred into HPLC vials.

***In-vitro* reconstitution of the *B. aryabhattai* SOS1 SFT pathway with recombinant enzymes.** Cloning of genes, and heterologous expression and purification of recombinant proteins *via* His-tag, was performed following a previously published protocol (**Felux et al., 2013**). The PCR primers used for directional cloning are listed in **Table S1**. PCR reaction mixtures consisted of 0.5-fold HF buffer (Thermo Fisher Scientific) containing 0.2 mM dNTP mix, 1 µM forward primer and 1 µM reverse primer, 5 ng genomic DNA of strain SOS1, and 20 U/ml Phusion High Fidelity DNA-Polymerase (Thermo Fisher Scientific). The PCR program for all genes was: initial denaturation at 98°C for 2 min; 25 cycles of 30 s denaturation at 98°C, 45 s annealing at 58°C, and 1.5 min elongation at 72°C; final elongation for 5 min at 72°C. PCR products were purified using the DNA Clean & Concentrator-5 kit (Zymo Research) and 5 ng of purified PCR product was used in the TOPO cloning reaction (Champion pET101 Directional TOPO Expression, Invitrogen). The cloning reaction was used to transform chemically competent *E. coli* NovaBlue (Novagen) for genes 1320, 1322, 1323 and 1325, and OneShot TOP 10 *E. coli* (Invitogen) for genes 1321 and 1323. The colony PCR reaction mixture

contained each 1 µM T7 forward and reverse primer (**Table S1**). The PCR program was: initial denaturation at 95°C for 10 min; 35 cycles of 45 s denaturation at 95°C, 45 s annealing at 55°C, and 1.5 min elongation at 72; final elongation step for 5 min at 72°C. Plasmids were prepared from overnight LB-liquid cultures (3.5 ml) containing 150 µg/ml ampicillin, using the Zyppy Plasmid Miniprep kit (Zymo Research). The correct inserts were confirmed by Sanger sequencing (Eurofins, Germany) using T7 primers (see above). The purified plasmids were used to transform chemical competent *E. coli* Rosetta 2 (DE3) (Invitrogen) according to Invitrogen's manual. For expression, transformands were grown in LB medium containing 100 µg/ml ampicillin and 35 µg/ml chloramphenicol, at 37°C and 200 rpm shaking, first in the 20-ml scale overnight and then in the 1-liter scale. These cultures were grown to an OD_{580nm} of 0.8-1.0. Then, IPTG (1 mM) was added to induce expression of the recombinant protein, and 3% (v/v) ethanol was added to induce chaperon formation (**Neidhardt et al., 1987; Thomas and Baneyx 1997**). After induction, the cultures were transferred to 15°C, 200 rpm shaking, for 24-25 h. Cells were harvested by centrifugation (15 min, 5000 x g, 4°C) and the cell pellets were stored at -20°C. Cells were resuspended in 2.5 ml of 10 mM imidazole buffer (pH 7.8) containing 1 U/ml DNase. Cell extracts were prepared by five passages through a French pressure cell (see above) and removal of the cell debris by centrifugation (15 min, 21.380 x g, 4°C). The overexpressed proteins were purified *via* His_6-tag through His SpinTrap columns (GE Healthcare Life Sciences); all centrifugation steps were performed at 200 x g for 30 sec at 4°C. For washing, 600 µl of 40 mM imidazole buffer (pH 7.8) and subsequently 600 µl of 60 mM imidazole buffer (pH 7.8) were used. The recombinant protein was eluted by adding three times 200 µl of 400 mM imidazole buffer (pH 7.8). The eluates were pooled and then desalted against 10 mM imidazole buffer (pH 7.8) (illustra NAP-10 gel filtration columns, GE Healthcare Life Sciences). Protein concentration in the recombinant protein preparations was determined by Bradford assay (see above). Enzymatic activities of the recombinantly produced enzymes was monitored by HPLC-MS in reactions containing 50 mM $(NH_4)_2CO_3$ buffer (pH 9.0), 1 mM

DTT, 1 mM $MnCl_2$, 0.5 mM $MgCl_2$ and 2 mM $^{13}C_6$-SQ, at room temperature. Optionally, 6 mM F6P or G6P or 12 mM GAP as acceptor was added. Thereafter, the assay was started by addition of SQ isomerase. Then, SF transaldolase was added, and finally, SLA dehydrogenase and 6 mM NAD^+. Before and after addition of each enzyme, samples were taken for HPLC-MS analysis (see above).

Photometric assays of SLA dehydrogenase activity. Recombinant SLA dehydrogenase activity was assayed photometrically using 10 µg/ml enzyme in 50 mM piperazine-N,N′-bis(2-ethanesulfonic acid) (PIPES) buffer (pH 6.8) containing 1 mM DTT, 1 mM $MnCl_2$, 0.5 mM $MgCl_2$, and NAD^+ or NADH in concentrations as specified below. The reduction of NAD^+ or oxidation of NADH was followed as absorbance at 365 nm in a spectrophotometer (Uvicon 922, Kontron Instruments); additionally, samples for HPLC-MS analysis of formation or disappearance of SL, SLA and/or DHPS were taken before, in between, and after the reactions (see above). Since we had no authentic SLA available as substrate, SLA was generated from DHPS (2 mM) in a reverse reaction of recombinant *E.coli* SLA reductase YihU (**Felux et al., 2015**, **Burrichter et al., 2018**) (1 µg/ml YihU; prepared as described previously, ref. **Denger et al., 2014**) in presence of NAD^+ (4 mM); subsequently, SLA dehydrogenase was added (100 µg/ml). A reverse reaction of SLA dehydrogenase 1325 (100 µg/ml) with SL (5 mM) and NADH (0.1 mM) was tested negative. For determination of promiscuous activities of the SLA dehydrogenase, GAP or E4P (6 mM) were used as substrates with NAD^+ (4 mM).

Isolation and genome sequencing of *Clostridium symbiosum* LT0011. *C. symbiosum* LT0011 was isolated from fecal material suspended in 30 mM bicarbonate buffer followed by serial dilution and plating on modified YCFA agar (sulfur compound- and short-chain fatty acid-free, 1.5% agar) (**Lopez-Siles et al., 2012**) supplemented with 10 mM SQ as the sole carbon and energy source. Colonies were streaked onto fresh plates and characterized by colony PCR and

sequencing of 16S rRNA genes (primers 8F and 1492R; **Table S1**). For genome sequencing, DNA was extracted using the Wizard Genomic DNA Purification KIT (Promega) and diluted to 0.1 ng/µl in 130 µl and sheared on a Covaris S220 Focused-ultrasonicator Instrument (Covaris, USA) to a target length of 350 bp. Library preparation was conducted according to the NEBNext Ultra II DNA Library Prep Kit for Illumina protocol (New England BioLabs). Indexing primers were ligated conforming to NEBNext Multiplex Oligos for Illumina manual (Index Primers Set 1, New England BioLabs). Samples were submitted for 150 bp paired-end sequencing on an Illumina HiSeq 3000/4000 at the Biomedical Sequencing Facility (BSF) of the Research Centre for Molecular Medicine (CeMM, Vienna, Austria). Additionally, a DNA library was prepared for MinION sequencing according to the manufacturer's protocol using a R9.4/FLO-MIN106 Flow Cell (Oxford Nanopore Rapid Sequencing, Oxford Nanopore Technologies, Oxford, UK). Illumina and Nanopore sequences were trimmed and filtered (> 100 bp and > 1 kb, respectively; PRINSEQlite v 0.20.4) (**Schmieder and Edwards 2011**). A hybrid assembly of both Illumina and Nanopore reads was performed using SPAdes (v.3.12.0) (**Bankevich et al., 2012**). Genome annotation was performed using PROKKA v.1.12 (**Seemann 2014**).

Cultivation of SQ-fermenting strains, total proteomics and detection of fermentation products. *Enterococcus gilvus* DSM15689 (**Tyrrell et al., 2002**) and *Eubacterium rectale* (*Agathobacter rectalis*) DSM17629 (**Duncan and Flint 2008**) were purchased from the Leibniz Institute DSMZ – German Collection of Microorganisms and Cell Cultures GmbH (Braunschweig). *Clostridium symbiosum* LT0011 (DSM180250) was isolated in this study (see above). For growth experiments and for generation of cell extracts for total proteomics (see above), the strains were grown anaerobically in a carbonate-buffered (pH 7.1) mineral salts medium reduced with 1 mM titanuim(III)nitriloacetate (Ti(III)-NTA) as reducing agent (basal medium, ref. **Widdel and Pfennig 1981**; trace elements solution, ref. **Widdel et al., 1983**; Ti(III)NTA solution, ref. **Moench and Zeikus 1983**; selenium-tungstate solution, ref.

Tschech and Pfennig 1984; vitamin solution, ref. **Pfennig 1978**) with 10 mM SQ and yeast extract (0.1% *w*/*v*) as supplement. The cultures were incubated in serum bottles enclosed with butyl-rubber stoppers under a N_2/CO_2 (80:20) gas atmosphere. Inoculation and sampling was done through the rubber stoppers with syringe and needle. Samples were taken at intervals for monitoring growth (OD580) (see above) and for HPLC analysis of SQ, DHPS and SL (see above). Short chain fatty acids and alcohols against authentic standards were analyzed on a HPLC system (system 10A, Shimadzu) with an Aminex column (HPX-87H, BioRad) and a refractive index detector (RID-10A, Shimadzu) at 60°C. The eluent was 5 mM H_2SO_4 at an isocratic flow of 0.6 ml/min. Under these conditions, the fermentation product acetate eluted at 11.7 min. This Aminex HPLC-RID method generally separates and detects carbohydrates, carboxylic acids, short-chain fatty acids, alcohols, ketones and other metabolites; no other products (peaks) than acetate were detected in any growth experiment. Hydrogen production was tested with a Peak Perfomer 1 (Peak Laboratories) trace gas analyzing gas chromatography system with a reducing compound photometer (RCP) detector; N_2 was used as carrier gas. For harvesting of the cultures, the serum bottles were opened and the cell suspension centrifuged under air atmosphere; the cell were disrupted, the cell extracts prepared, and the total proteomic analyses were done as, described above in the appropriate sections for *B. aryabhattai* SOS1.

SUPPLEMENTAL REFERENCES

Bankevich, A., S. Nurk, D. Antipov, A. A. Gurevich, M. Dvorkin, A. S. Kulikov, V. M. Lesin, S. I. Nikolenko, S. Pham, A. D. Prjibelski, A. V. Pyshkin, A. V. Sirotkin, N. Vyahhi, G. Tesler, M. A. Alekseyev and P. A. Pevzner (2012). "SPAdes: a new genome assembly algorithm and its applications to single-cell sequencing." Journal of Computational Biology **19**(5): 455-477.

Bolger, A. M., M. Lohse and B. Usadel (2014). "Trimmomatic: a flexible trimmer for Illumina sequence data." Bioinformatics **30**(15): 2114-2120.

Bradford, M. M. (1976). "A rapid and sensitive method for the quantitation of microgram quantities of protein utilizing the principle of protein-dye binding." Analytical Biochemistry **72**(1): 248-254.

Burrichter, A., K. Denger, P. Franchini, T. Huhn, N. Müller, D. Spiteller and D. Schleheck (2018). "Anaerobic degradation of the plant sugar sulfoquinovose concomitant with H2S production: *Escherichia coli* K-12 and *Desulfovibrio* sp. strain DF1 as co-culture model." Frontiers in Microbiology **9**: 2792-2792.

de Souza, L. M., M. Müller-Santos, M. Iacomini, P. A. J. Gorin and G. L. Sassaki (2009). "Positive and negative tandem mass spectrometric fingerprints of lipids from the halophilic Archaea *Haloarcula marismortui*." Journal of Lipid Research **50**(7): 1363-1373.

Denger, K., T. Huhn, K. Hollemeyer, D. Schleheck and A. M. Cook (2012). "Sulfoquinovose degraded by pure cultures of bacteria with release of C3-organosulfonates: complete degradation in two-member communities." FEMS Microbiolgy Letters **328**(1): 39-45.

Denger, K., M. Weiss, A. K. Felux, A. Schneider, C. Mayer, D. Spiteller, T. Huhn, A. M. Cook and D. Schleheck (2014). "Sulphoglycolysis in *Escherichia coli* K-12 closes a gap in the biogeochemical sulphur cycle." Nature **507**: 114-117.

Duncan, S. H. and H. J. Flint (2008). "Proposal of a neotype strain (A1-86) for *Eubacterium rectale*. Request for an Opinion." International Journal of Systematic and Evolutionary Microbiology **58**(7): 1735-1736.

Felux, A.-K., K. Denger, M. Weiss, A. M. Cook and D. Schleheck (2013). "*Paracoccus denitrificans* PD1222 utilizes hypotaurine via transamination followed by spontaneous desulfination to yield acetaldehyde and, finally, acetate for growth." Journal of Bacteriology **195**(12): 2921-2930.

Felux, A.-K., D. Spiteller, J. Klebensberger and D. Schleheck (2015). "Entner-Doudoroff pathway for sulfoquinovose degradation in *Pseudomonas putida* SQ1." Proceedings of the National Academy of Sciences **112**(31): E4298-E4305.

Kennedy, S. and C. Fewson (1968). "Enzymes of the mandelate pathway in bacterium NCIB 8250." Biochemical Journal **107**(4): 497.

Kolmogorov, M., B. Raney, B. Paten and S. Pham (2014). "Ragout - a reference-assisted assembly tool for bacterial genomes." Bioinformatics **30**(12): i302-309.

Lopez-Siles, M., T. M. Khan, S. H. Duncan, H. J. Harmsen, L. J. Garcia-Gil and H. J. Flint (2012). "Cultured representatives of two major phylogroups of human colonic *Faecalibacterium prausnitzii* can utilize pectin, uronic acids, and host-derived substrates for growth." Applied and Environmental Microbiology **78**(2): 420-428.

Luo, R., B. Liu, Y. Xie, Z. Li, W. Huang, J. Yuan, G. He, Y. Chen, Q. Pan, Y. Liu, J. Tang, G. Wu, H. Zhang, Y. Shi, C. Yu, B. Wang, Y. Lu, C. Han, D. W. Cheung, S. M. Yiu, S. Peng, Z. Xiaoqian, G. Liu, X. Liao, Y. Li, H. Yang, J. Wang and T. W. Lam (2012). "SOAPdenovo2: an empirically improved memory-efficient short-read de novo assembler." Gigascience **1**(1): 18.

Mayer, J., T. Huhn, M. Habeck, K. Denger, K. Hollemeyer and A. M. Cook (2010). "2,3-Dihydroxypropane-1-sulfonate degraded by *Cupriavidus pinatubonensis* JMP134: purification of dihydroxypropanesulfonate 3-dehydrogenase." Microbiology **156**(5): 1556-1564.

Moench, T. T. and J. G. Zeikus (1983). "An improved preparation method for a titanium (III) media reductant." Journal of Microbiological Methods **1**(4): 199-202.

Neidhardt, F. C., J. L. Ingraham, K. B. Low, B. Magasanik, M. Schaechter and H. Umbarger (1987). *Escherichia coli* and *Salmonella typhimurium*: cellular and molecular biology, American Society for Microbiology Washington, DC.

Peck, S. C., K. Denger, A. Burrichter, S. M. Irwin, E. P. Balskus and D. Schleheck (2019). "A glycyl radical enzyme enables hydrogen sulfide production by the human intestinal bacterium *Bilophila wadsworthia*." Proceedings of the National Academy of Sciences **116**(8): 3171-3176.

Pfennig, N. (1978). "*Rhodocyclus purpureus gen. nov*. and *sp. nov.*, a ring-shaped, vitamin B12-requiring member of the family *Rhodospirillaceae*." Int. J. Syst. Evol. Microbiol. **28**(2): 283-288.

Schmidt, A., N. Müller, B. Schink and D. Schleheck (2013). "A Proteomic view at the biochemistry of syntrophic butyrate oxidation in *Syntrophomonas wolfei*." PLOS ONE **8**(2): e56905.

Schmieder, R. and R. Edwards (2011). "Quality control and preprocessing of metagenomic datasets." Bioinformatics **27**: 863-864.

Seemann, T. (2014). "Prokka: rapid prokaryotic genome annotation." Bioinformatics **30**(14): 2068-2069.

Styp von Rekowski, K. , K. Denger and A.M. Cook (2005). "Isethionate as a product from taurine during nitrogen-limited growth of *Klebsiella oxytoca* TauN1." Archives of Microbiology **183**: 325-330.

Thomas, J. G. and F. Baneyx (1997). "Divergent effects of chaperone overexpression and ethanol supplementation on inclusion body formation in recombinant *Escherichia coli*." Protein Expression and Purification **11**(3): 289-296.

Thurnheer, T., T. Köhler, A. M. Cook and T. Leisinger (1986). "Orthanilic acid and analogues as carbon sources for bacteria: growth physiology and enzymic desulphonation." Microbiology **132**(5): 1215-1220.

Tschech, A. and N. Pfennig (1984). "Growth yield increase linked to caffeate reduction in *Acetobacterium woodii*." Arch. Microbiol. **137**: 163-167.

Tyrrell, G. J., L. Turnbull, L. M. Teixeira, J. Lefebvre, M. d. G. S. Carvalho, R. R. Facklam and M. Lovgren (2002). "*Enterococcus gilvus* sp. nov. and *Enterococcus pallens* sp. nov. isolated from human clinical specimens." Journal of Clinical Microbiology **40**(4): 1140-1145.

Widdel, F., G.-W. Kohring and F. Mayer (1983). "Studies on dissimilatory sulfate-reducing bacteria that decompose fatty acids III. Characterization of the filamentous gliding *Desulfonema limicola gen. nov. sp. nov*., and *Desulfonema magnum sp. nov.*" Arch. Microbiol. **134**(4): 286-294.

Widdel, F. and N. Pfennig (1981). "Studies on dissimilatory sulfate-reducing bacteria that decompose fatty acids. I. Isolation of new sulfate-reducing bacteria enriched with acetate from saline environments. Description of *Desulfobacter postgatei gen. nov., sp. nov*." Arch. Microbiol. **129**(5): 395-400.

William, S., H. Feil and A. Copeland (2012). "Bacterial genomic DNA isolation using CTAB." Sigma **50**: 6876.